Escola Superior de Tecnologia da Saúde do Porto

Instituto Politécnico do Porto

Melissa Sofia Figueiredo Couto

Molecular and biochemical mechanisms involved in the toxicity of a marine cyanobacteria compound on cancer cell lines

Dissertação submetida à Escola Superior de Tecnologia da Saúde do Porto para cumprimento dos requisitos necessários à obtenção do grau de Mestre em Bioquímica em Saúde, realizada sob a orientação Professora Doutora Maria do Rosário Fidalgo Martins, Departamento das Ciências Morfológicas na ESTSP do Instituto Politécnico do Porto e Centro Interdisciplinar de Investigação Marinha e Ambiental (CIIMAR), coorientação Professor Doutor Ralph Urbatzka, Centro Interdisciplinar de Investigação Marinha e Ambiental (CIIMAR) e orientação tutorial Professora Doutora Cristina Prudêncio, Departamento das Ciências Químicas e das Biomoléculas na ESTSP do Instituto Politécnico do Porto.

.

Setembro de 2015

Molecular and biochemical mechanisms involved in the toxicity of a marine cyanobacteria compound on cancer cell lines

Dedicatory

I dedicate this work to the memory of people who are no longer here to see me reach another stage in my academic life.

Agostinho Lima

Jorge Couto

Nazário Couto

Molecular and biochemical mechanisms involved in the toxicity of a marine cyanobacteria compound on cancer cell lines

Acknowledgements

For this work had the support and understanding of many people, which would like to thank you for everything did for me and without which this work would not have been realized.

I would like to thank the Escola Superior de Tecnologia da Saúde do Porto, especially the Area of Chemistry and Biomolecules and the Area of Morphological Sciences.

To Professor Doctor Rúben Fernandes and Professor Doctor Cristina Prudêncio by always having believed in my potential and for all the support provided.

To Professor Doctor Rosário Martins and Professor Doctor Ralph Urbatzka for help, sharing of knowledge and the patience to teach me new things along this thesis.

To Susana Moutinho for to have me integrated into the laboratory Morphological Sciences, taught everything I needed and has become a good friend.

I would also like to thank all members of LEGE (Laboratory of Ecotoxicology, Genomics and Evolution) team for the good work environment at work and for always being available to help me, especially to Sara Freitas for having taught me everything I needed to prepare this work, to Tiago Afonso for having me provided all the information and help in continuing its work, to Tiago Ribeiro to be always available. Also to Micaela Vale, João Morais, Mariana Carneiro, Pedro Leão, Raquel Castelo-Branco, Sofia Costa, Mafalda Castro, Marco Preto and Alexander Campos. To Professor Doctor Vítor Vasconcelos for accepting me in the laboratory for the realization of my master's thesis.

To my master colleagues for sharing with me two fantastic years. Especially to Marta Gonçalves, Sofia Cabral, Joana Correia, Salome Monteiro, Anita Campos and Nuno Durães to be more than colleagues, they are friends for all times.

To my friends Marina Gomes, Ana Miranda, Ana Silva and Andreia Garcia for supporting me in another stage of my academic life and understand my absence.

To my fiancé Marcelo Lopes for supporting me, for not letting me give up, to always have a comforting word and all patience.

Finally, I would like to thank my parents and my grandparents because without them would not have been possible to carry out this master. Always supported me in my

decisions and always understood what this meant academic stage, not be much time as you like with them.

This research was partially supported by the Strategic Funding UID/Multi/04423/2013 through national funds provided by FCT – Foundation for Science and Technology and European Regional Development Fund (ERDF), in the framework of the programme PT2020 and by the Project MARBIOTECH (reference NORTE-07-0124-FEDER-000047) within the SR&TD Integrated Program MARVALOR - Building research and innovation capacity for improved management and valorization of marine resources, supported by the Programa Operacional Regional do Norte (ON.2 – O Novo Norte) and by the European Regional Development Fund.

Resumo

Nos últimos anos a biotecnologia marinha tem revelado um papel crucial no futuro da bioindústria. Entre os muitos recursos marinhos, as cianobactérias têm revelado um grande potencial na produção de compostos bioativos com diversas aplicabilidades. O potencial farmacológico destes organismos tem sido uma das áreas mais exploradas nomeadamente o seu potencial antibacteriano, antifúngico e anticancerígeno. Este trabalho teve por base a avaliação do potencial anticancerígeno do composto E13010 F 5.4 isolado da estirpe de cianobacteria marinha *Synechocystis salina* LEGE 06099. Pretendeu-se assim explorar mecanismos moleculares e bioquímicos subjacentes à bioatividade detetada em células cancerígenas humanas, especificamente nas linhagens de carcinoma do cólon RKO e HT-29.

O isolamento do composto foi realizado a partir de biomassa da estirpe de cianobactéria, obtida por cultura em grande escala. Para obtenção do composto procedeu-se ao fracionamento, confirmação e isolamento por ressonância magnética nuclear (RMN), cromatografia em camada fina (TLC) e cromatografia líquida de alta eficiência (HPLC).
Foram realizados ensaios de viabilidade celular baseados na redução do brometo 3-(4.5-dimetiltiaziol-2-il)-2.5-difeniltetrazolio (MTT) para avaliar o potencial citotóxico do composto. Da bateria de linhagens celulares RKO (carcinoma do cólon), HT-29 (adenocarcinoma colorretal), MG-63 (osteossarcoma) e T47D (carcinoma da mama) foram selecionadas as linhas celulares RKO e HT-29 para elucidação dos mecanismos de citotoxicidade.

Para a avaliação dos mecanismos envolvidos na citotoxicidade as linhagens celulares RKO e HT-29 formam expostas ao composto e foi realizada uma bordagem em termos de genómica por expressão de mRNA de genes envolvidos na apoptose e ciclo celular por PCR em Tempo Real e uma abordagem em termos de proteómica por separação de proteínas por eletroforese bidimensional (2DE). Para a expressão de mRNA foram selecionados os genes RPL8, HPRT1, VDAC, SHMT2, CCNE, CCNB1, P21CIP, BCL-2 e BAD, para proteómica os pontos isoeléctricos entre 3 – 10 e massas moleculares de 19 - 117 kDa foram separados por géis de poliacrilamida (2DGE).

Os resultados do MTT confirmaram a redução da viabilidade celular. Os resultados de RT-PCR para a expressão de genes estudados não se mostraram completamente elucidativas.

Para a linhagem celular RKO verificou-se uma redução na expressão do gene P21CIP, uma tendência para a redução na expressão do gene BAD e um aumento na expressão do gene CCNB1, o que aponta para um esforço pela proliferação celular. Na linhagem HT-29 verificou-se um aumento na expressão do P21CIP e BAD o que poderá explicar a redução da viabilidade celular. Os resultados de 2DGE apontam para padrões de proteómica com alterações nos diferentes *spots* nas células tratadas e no controlo com diferenças qualitativas e quantitativas, e diferenças na resposta entre RKO e HT-29.

Palavras Chave: cianobactéria, picocianobactéria, *Synechocystis salina*, potencial anticancerígeno, genómica, proteómica

Abstract

In recent years marine biotechnology has revealed a crucial role in the future of bioindustry. Among the many marine resources, cyanobacteria have shown great potential in the production of bioactive compounds with diverse applicability. The pharmacological potential of these organisms has been one of the most explored areas in particular its antibacterial, antifungal and anticancer potential. This work was based on the assessment of potential anticancer compound E13010 F 5.4 isolated from marine cyanobacteria strain *Synechocystis salina* LEGE 06099. Thus the aim of this work was to explore molecular and biochemical mechanisms underlying the bioactivity detected in human cancer cells, specifically in lines RKO colon carcinoma and HT-29.

The isolation of the compound was performed from biomass obtained by large-scale culture. To obtain the compound fractionation was carried and confirmation and isolation performed by Nuclear Magnetic Resonance (NMR), Thin Layer Chromatography (TLC) and High-Performance Liquid Chromatography (HPLC).

Cell viability assays were performed based on reduction of 3- (4,5-dimetiltiaziol-2-yl) -2,5-diphenyltetrazolium bromide (MTT) to assess the cytotoxic potential of the compound. From the battery of cell lines RKO (colon carcinoma), HT-29 (colorectal adenocarcinoma), MG-63 (osteosarcoma) and T47D (breast carcinoma) the cell lines RKO and HT-29 were selected for elucidation of mechanisms of cytotoxicity.

For the elucidation of the mechanisms involved in cytotoxicity the cell lines RKO and HT29 were exposed to the compound. A genomic approach based in the mRNA expression of genes involved in apoptosis and cell cycle by Real-Time PCR and a proteomic approach based on the separation of proteins by two-dimensional electrophoresis (2DGE) was performed. For mRNA expression were selected the genes RPL8, HPRT1, VDAC, SHMT2, CCNE, CCNB1, P21CIP, BCL-2 and BAD and for proteomics isoelectric focussing between 3 – 10 and molecular weight of 19 – 117 kDa separated by polyacrylamide gels (2DGE).

The MTT results confirmed the reduction of the cell viability. The RT-PCR results for the expression of genes studied were not yet fully elucidative. For the cell line RKO there was a significant reduction in the expression of the gene P21CIP, and a tendency for reduction in the BAD gene expression and for increased expression of gene CCNB1, pointing to an

effort for cell proliferation. In HT-29 cell line, there was a tendency for increase in the expression of P21CIP and BAD, which may explain the reduction in cell viability. The 2DGE results indicate proteomic patterns with differentially altered spots in the treated and control cells with both qualitative and quantitative differences, and differences in response between the RKO and HT-29 cell lines.

Key word: cyanobacteria, picocyanobacteria, *Synechocystis salina*, anticancer potential, genomics, proteomics

Table of Contents

List of abbreviations

2DGE – Two-dimensional electrophoresis

ACN – Acetonitrile

ATCC – American Type Culture Collection

BAD – BCL2-Associated Agonist Of Cell Death

BCL-2 – B-Cell CLL/Lymphoma

BPB – Bromophenol Blue

CCNB1 – Cyclin B1

CCNE – Cyclin E1

cDNA – Complementary DNA

CEMUP – Centro de Materiais da Universidade do Porto

CHAPS – 3-[(3-Cholamidopropyl)-dimethylammonio]-1-propane sulfonate

CIIMAR – Center of Marine and Environmental Research

CID – Collision-induced Dissociation

CRC – Colorectal cancer

DCM – Dichloromethane

DMEM – Dulbecco's Modified Eagle Medium

DMSO – Dimethyl sulfoxide

DNA – Deoxyribonucleic acid

DTT – Dithiothreitol

EnoA – Alpha-enolase

ER – endoplasmic reticulum

EtOAc – Ethyl acetate

GRP78 – 78 kDa glucose-regulated protein

GRP – glucose-regulated proteins

Hex – Hexane

HPRT1 – Hypoxanthine Phosphoribosyltransferase

HT-29 – Human colorectal adenocarcinoma cell line

IEF – First-dimension isoelectric focusing

IPATIMUP – Institute of Molecular Pathology and Immunology at the University of Porto

LEGE – Laboratory of Ecotoxicology, Genomics and Evolution

MALDI-TOF/TOF – Matrix-assisted laser desorption ionization time-of-flight/time-of-flight

MeOH – Methanol

MG-63 – Human osteossarcoma cell line

mRNA – Messenger RNA

MTT – 3-(4.5-dimethylthiazol-2-yl)-2.5-diphenyltetrazolium bromide

NMR – Nuclear Magnetic Resonance spectroscopy

NTC – Negative control

P21CIP – Cyclin-Dependent Kinase Inhibitor 1A

PBS – Phosphate Buffered Saline

PCR – Polymerase Chain Reaction

PKS – Polyketide Synthetase

PMA DIP – Phosphomolybdic acid

RB flasks – Round bottom flasks

RKO – Human colon carcinoma cell line

RNA – Ribonucleic acid

RPL8 – Ribosomal Protein L8

RT-PCR – Real-Time Polymerase Chain Reaction

SB – Solubilisation Buffer

SDS-PAGE – Sodium Dodecyl Sulphate Polyacrylamide gel electrophoresis

SHMT2 – Serine hydroxymethy transferase 2

SH-SY5Y – Human neuroblastoma cell line

T47D – Human ductal breast epitelial tumor cell line

TEMED – Tetramethylethylenediamine

TFA – Trifluoroacetic acid

TLC – Thin Layer Chromatography

UV – Ultraviolet light

VDAC – Voltage-dependent anion channel

VLC – Vacuum liquid chromatography

Figure Index

Table Index

Chapter I – Introduction

I. Introduction

1. Cyanobacteria: generalities

The cyanobacteria (blue–green algae) are important primary producers of marine, estuarine and fresh water ecosystems and producers of active secondary metabolites that range from toxins, to allelopatic compounds and compounds with pharmacological potential (1-4).

Cyanobacteria are photoautotrophic gram-negative prokaryotes with the capacity to perform oxygenic photosynthesis, nitrogen fixation and carbon recycling. In fact, cyanobacteria are very important in biogeochemical cycles, as they are responsible for about 30% of global primary production, especially in the central oceans (5).

Cyanobacteria are an ancient monophyletic phylum of the Bacteria domain. It is considered that these organisms developed oxygenic photosynthesis 2.5–3.5 billion years ago and this capacity was subsequently transferred into eukaryotes via endosymbiosis, leading to the appearance of eukaryotic algae and plants (5-7). Latest genome analyses seem to point that the primary endosymbiont was most closely related to the current filamentous strains (5, 8). As cyanobacteria are photoautotrophic organisms, they only need light, water and some inorganic nutrients. As a result, cyanobacteria became dominant organisms with major impacts on geochemical processes of our planet. During the massive development of cyanobacteria, oxygen was generated in the atmosphere, which enabled the rise of oxygen-dependent organisms that exists today. This wide range of habitats reflects the impressive capability of cyanobacteria to acclimate to changes of many different environmental factors (5, 9). Probably the reason to adapt is based on the simple genome (catching many mutations) and the asexual reproduction mode and inhabiting a multiplicity of environments worldwide, a result of its morphological and physiological diversity (1, 2, 10).

Taxonomically the cyanobacteria can be classified “botanical” or “bacterial” (10). The actualized taxonomic botanical system of classification uses morphological, biochemical and molecular characters, cyanobacteria has been grouped into five orders, *Chroococcales* (subsections I), *Pleurocapsales* (subsections II), *Oscillatoriales* (subsections III), *Nostocales* (subsections IV) and *Stigonematales* (subsections V), with correspondence to the five subsections proposed in the Bergey’s Manual of Systematic (10-13).

Cyanobacteria correspondent to subsections I and II are unicellular. The subsections I are divided by binary fission, however the subsections II are multiple fission. The subsections III, a few filamentous strains, they have not cell differentiation. Although, the subsections IV and V (filamentous strains, have a capacity to differentiated in heterocysts and akinetes. The subsections V are capable to divide in multiple planes (10).

In the last years marine biotechnology has revealed to be a crucial key in future bioindustry (14). Among many marine resources, cyanobacteria have a great importance in marine biotechnology, namely due to the high potential in producing potential pharmacological compounds such as antiviral (12, 15-17), antibacterial, antifungal and anticancer (Table 1) (1, 18). Natural products are screened frequently for the treatment of various diseases, including marine products. Some marine compounds were approved by the Food and Drug Administration (FDA) for treatment of various cancers; among the FDA approved compounds are anticancer agent derived from cyanobacteria, and several other compounds from cyanobacteria are in different phases of clinical trials (19). Cyanobacteria are also known for their role in the nutrient cycling and are therefore very important in ecosystems poor in nutrients both in freshwater and sea (14, 20).

Morphologically, cyanobacteria are surrounded by two membranes. The cell wall is enclosed by an outer membrane that surrounds the periplasmic space, whereas the cytoplasmic membrane surrounds the cytoplasm. Inside the cytoplasm, it has a third membrane system, a thylakoid membrane that has the photosynthetic complexes. Furthermore, the respiratory electron transport chain is also mostly situated at the thylakoid membranes (5).

Table 1 Marine cyanobacterial compounds with potential anticancer properties. Adapted from *Costa et al.*, 2012 (18).

Compound	Source	Class of compound	Anticancer activity	References
Ankaraholide A	*Geitlerinema*	Glycosilated swinholide	Lung cancer and breast carcinoma	(21)
Apratoxin A	*Lyngbya majuscula*	Cyclic depsipeptide	Oral epidermoid cancer, colon cancer, osteosarcoma and cervical carcinoma	(22-24)
Apratoxins B–C	*Lyngbya* sp.	Cyclic depsipeptide	Oral epidermoid cancer and colon cancer	(22)
Apratoxin D	*Lyngbya majuscula* and *Lyngbya sordida*	Cyclic depsipeptide	Lung cancer	(25)
Apratoxin E	*Lyngbya bouilloni*	Cyclic depsipeptide	Osteosarcoma, colon adenocarcinoma and epithelial carcinoma	(24)
Apratoxins F–G	*Lyngbya bouilloni*	Cyclic depsipeptide	Lung cancer and colorectal cancer	
Aurilide B	*Lyngbya majuscula*	Cyclic depsipeptide	Lung cancer	
Aurilide C	*Lyngbya majuscula*	Cyclic depsipeptide	Lung cancer	(26)
Belamide A	*Symploca* sp.	Linear tetrapeptide	Colon cancer	(26)
Bisebromoamide	*Lyngbya* sp.	Peptide	Epithelial carcinoma	(27)
Biselyngbyaside	*Lyngbya* sp.	Glicomacrolide	Epithelial carcinoma, central nervous system cancer and lung cancer	(28)
Calothrixin A	*Calothrix*	Pentacyclic Indolophenanthridine	Epithelial carcinoma and leukemia	(29)
Calothrixin B	*Calothrix*	Pentacyclic Indolophenanthridine	Epithelial carcinoma and leukemia	(30)
Caylobolide A	*Lyngbya majuscula*	Macrolactone	Colon carcinoma	(31, 32)
Caylobolide B	*Phormidium* spp.	Macrolactone	Colorectal adenocarcinoma and cervical carcinoma	(32, 33)

Coibamide A	*Leptolyngbya* sp.	Cyclic depsipeptide	Lung cancer, breast cancer, melanoma, leukemia and astrocytoma	(34)
Cryptophycin 1	*Nostoc* spp.	Cyclic depsipeptide	Mammary adenocarcinoma, mammary carcinoma, ovarian carcinoma, leukemia, colon carcinoma and cervical carcinoma	(34, 35)
Dolastatin 10	*Symploca* sp.	Linear Pentapeptide	Lung carcinoma, prostate cancer, lymphoma and leukemia	(36-39)
Dolastatin 12	*Leptolyngbya* sp.	Cyclic depsipeptide	Lung carcinoma	(36)
Dragonamide	*Lyngbya majuscula*	Lipopeptide	Lung epithelial adenocarcinoma, colon adenocarcinoma and melanoma	(36)
Ethyl Tumonoate A	*Oscillatoria margaritifera*	Peptide	Lung cancer	(40)
Hoiamide A	Assemblage of *Lyngbya majuscule and Phormidium* gracile	Cyclic depsipeptide	Lung cancer	(41)
Hoiamide B	Cyanobacterial sample	Cyclic depsipeptide	Lung cancer	(41)
Homodolastatin 16	*Lyngbya majuscula*	Cyclic depsipeptide	Esophageal cancer and cervical cancer	(42)
Isomalyngamide A and A-1	*Lyngbya majuscula*	Fatty acid amides	Breast cancer	(43)
Jamaicamides A – C	*Lyngbya majuscula*	Polyketide-Peptides	Lung cancer	(44)
Kalkitoxin	*Lyngbya majuscula*	Lipopeptide	Colon carcinoma	(45)
Lagunamide C	*Lyngbya majuscula*	Cyclic depsipeptide	Lung adenocarcinoma, prostate cancer, ileocecal, colorectal cancer and ovary cancer	(46)

Largazole	*Symploca* sp.	Cyclic depsipeptide	Breast cancer, osteosarcoma, lung cancer and colorectal carcinoma	(46, 47)
Lyngbyabellin A	*Lyngbya majuscula*	Cyclic depsipeptide	Nasopharyngeal carcinoma and colon adenocarcinoma	(36, 48)
Lyngbyaloside	*Lyngbya* sp.	Glicomacrolide	Nasopharyngeal carcinoma and colon adenocarcinoma	(49)
Majusculamide C	*Lyngbya majuscula*	Cyclic depsipeptide	Ovarian carcinoma, kidney cancer, lung cancer, colorectal cancer and gliobastoma	(50)
Malevamide D	*Symploca hydnoides*	Peptide ester	Lung cancer, colon cancer and melanoma	(51)
Malyngamide 2	*Lyngbya sordida*	Fatty acid amine	Lung cancer	(52)
Malyngamide C, J and K	*Lyngbya majuscula*	Fatty acid amine	Lung cancer	(53)
Malyngolide dimmer	*Lyngbya majuscula*	Cyclodepside	Lung cancer	(54)
Nostocyclopepti-de A1 and A2	*Nostoc* sp.	Cyclic heptapeptides	Oral epidermoid cancer and colon cancer	(55)
Obyanamide	*Lyngbya confervoides*	Cyclic heptapeptides	Oral epidermoid cancer and colon cancer	(56)
Palauamide	*Lyngbya* sp.	Cyclic depsipeptide	Cervical carcinoma, lung adenocarcinoma, gastrocarcinoma and oral epidermoid cancer	(57, 58)
Palmyramide A	*Lyngbya majuscula*	Cyclic depsipeptide	Lung cancer	(59)
Pitipeptolides A–B	*Lyngbya majuscula*	Cyclic depsipeptide	Colon cancer, colon adenocarcinoma and breast cancer	(60, 61)
Pitipeptolide C	*Lyngbya majuscula*	Cyclic depsipeptide	Colon cancer, colon adenocarcinoma	(61)

			and breast cancer	
Pitiprolamide	*Lyngbya majuscula*	Cyclic depsipeptide	Colorectal carcinoma and breast adenocarcinoma	(62)
Pseudodysidenin	*Lyngbya majuscula*	Lipopeptide	Lung adenocarcinoma, colon adenocarcinoma and melanoma	(63)
Somocystinamide A	*Lyngbya majuscula*	Lipopeptide	Leukemia, lung carcinoma, melanoma and myeloma	(64)
Symplocamide	*Symploca* sp.	Cyclic peptide	Lung cancer	(65)
Symplostatin 1	*Symploca hydnoides*	Linear Pentapeptide	Breast carcinoma, ovarian carcinoma and epidermoid carcinoma	(66, 67)
Tasiamide	*Symploca* sp.	Cyclic peptide	Oral epidermoid cancer and colon cancer	(68)
Tasiamide B	*Symploca* sp.	Peptide	Oral epidermoid cancer	(69)
Tasipeptins A-B	*Symploca* sp.	Cyclic depsipeptides	Oral epidermoid cancer	(70)
Ulongapeptin	*Lyngbya* sp.	Cyclic depsipeptides	Oral epidermoid cancer	(71)
Veraguamides A-G	*Symploca cf. Hydnoides*	Cyclic depsipeptides	Lung cancer	(72)
Wewakazole	*Lyngbya sórdida*	Cyclic depsipeptides	Lung cancer	(52)
Wewakpeptins	*Lyngbya semiplena*	Depsipeptides	Lung cancer	(73)

1.1. Picocyanobacteria

Picoplankton is constituted by organisms with a size range between 0.2 and 2 μm (21, 22). Small unicellular cyanobacteria in the size range of picoplankton represent ubiquitous components of pelagic ecosystems (23) where they contribute substantially to both phytoplankton biomass and production in marine and freshwater ecosystems (24). This small organisms are found in large quantities in both freshwater and marine water throughout the world (25, 26) and includes prokaryotic and eukaryotic autotrophs and

heterotrophs being the predominant constituents, the cyanobacteria and heterotrophic bacteria. Picophytoplankton is responsible for most of the total primary production in lakes and oceans (27) and the production of heterotrophic bacteria is often related to this primary production (28, 29).

Picoplanktonic cyanobacteria include isolates of the *Chroococcales* order, particularly the picocyanobacterial genera *Cyanobium*, *Prochlorococcus, Synechocysti* and *Synechococcus*. *Cyanobium* consists of solitary oval cells without gelatinous envelopes. Most small cyanobacteria rod that exist in natural freshwater or marine plankton are classified into *Synechococcus* group and are identified as *Synechococcus* sp. or *Cyanobium* sp.. According Rippka et al (30) the genus *Cyanobium* was secreted from *Synechococcus* based of different mean DNA base composition and sensitivity to various cyanophages. This proves that exist a close relationship between *Cyanobium* and *Synechococcus*. Cell division proceeds by perpendicular binary fission (usually cleavage), which is sometimes asymmetrical (22). The genus marine *Synechococcus* is very common in all oceans, for this reason is the base of the marine food web because it is the primary food producers in coastal environments (31).

Prochlorococcus, like *Synechococcus*, also exists in large quantities in the oceans. They are unicellular and have different photosynthetic pigments. Its strains are phenotypically distinct and many have not yet been described (32-35).

Marine picoplanktonic cyanobacteria are extremely difficult to isolate. For this reason, several methods have been used to obtain axenic clonal cultures: UV radiation, chemical treatments using phenol, antibiotics and sulfide, and physical treatments such as micropipette washing or plating methods (36-40). Picocyanobacteria are more easily isolated using agarose and low-melting temperature agarose to obtain colonies of picoplanktonic cyanobacteria and their axenic clonal cultures from unialgal bacterized cultures by plating method (21).

1.1.1. Picocyanobacteria bioactive potential

In the last years marine cyanobacteria have been in the frontline for the isolation of bioactive compounds. Also it is currently using natural sources such as marine products to produce new complexes drugs (41, 42). The interest on marine biotechnology was enhanced by the results of some studies, which indicated that marine microorganisms are

substantially involved in the biosynthesis of marine natural products previously isolated from macroorganisms such as invertebrates (43, 44). The cultivated marine microorganisms, particularly actinomycetes and fungi, are well known for their production of bioactive metabolites (45). Cyanobacteria (blue-green algae) are also identified as a promising source of biochemically active natural products (46, 47).

Cyanobacteria produce a wide variety of secondary metabolites that exhibit a variety of biological activities and chemical structures. On one hand, some cyanobacterial secondary metabolites may have toxic effects on living organisms, such as common toxins like microcystins (48, 49) or may have ecological roles such as allelopathy and may be used for biotechnological applications such as algaecides, herbicides and insecticides (50). On the other hand, cyanobacteria have become a new source of active compounds showing interesting biological activities ranging from antibiotics, immunosuppressants, anticancer, antiviral and anti-inflammatory to proteinase-inhibiting agents (48, 49, 51). Studies oriented to the production of compounds that could be used as antibiotics and drugs against important diseases such as cancer found that cyanobacteria strains of the genera *Synechocystis* and *Synechococcus* caused growth inhibition of Gram-positive bacteria (52) and apoptotic effects against the myelogenic human leukaemia cell line HL-60 and in the human neuroblastoma cell line SH-SY5Y (3). In all the reported cases, although the bioactive compounds were not identified, the results support the hypothesis that picocyanobacteria also produce biologically active compounds.

The toxins of cyanobacteria constitute a most important source of natural product toxins that are found in surface supplies of both freshwater and seawater (53-55). Marine cyanobacteria have been extensively studied for the production of compounds with pharmacological applications (56), however, until a few years studies mainly focused on large filamentous forms (57). In the last years a considerable effort has been applied in the study of picocyanobacteria as a source of bioactive compounds (3). In contrast to filamentous forms, picoplanktonic cyanobacteria occur in low densities under normal conditions and thus have been largely overlooked for biological activities.

Bioassays-guided fractionation is a methodology that has been efficaciously used for the isolation and identification of marine natural compounds, since it allows the rapid recognition of the active fractions, which may contain compounds of interest (3, 58-60). Based on this methodology several picocyanobacteria strains revealed potential as a source

of bioactivity interesting compounds. In Table 2 a compilation of bioactivities of picocyanobacteria is shown based on scientific literature.

Table 2 Bioactivities described to picocyanobacteria.

Genera	Origin	Bioactivity	Assay	Model tested	References
Synechococcus sp.	Temperate coastal	Neurological and behavioural changes	Light-dark preference test (scototaxic test), is a method to measure anxiety in fish and whether pharmacological compound alter anxiety	Black perch (*Embiotoca jacksoni*)	(31)
Cyanobium sp. LEGE 06098	Portuguese Coast	Anticancer activity	MTT and LDH	Cancer cell lines	(3)
		Toxicity and developmental toxicity	*Artemia salina* mortality and embryonic development of *Paracentrotus lividus*	*Artemia salina* *Paracentrotus lividus*	(61)
Cyanobium sp. LEGE06113		Anticancer activity	MTT and LDH	Cancer cell lines	(3)
		Antitumour activity of hierridin B, a secondary metabolite		Hepatocellular carcinoma cell line HepG2, colon adenocarcinoma cell line HT-29, neuroblastoma cell line SH-SY5Y, breast carcinoma cell line T47D, normal prostate cell line PNT2, breast adenocarcinoma SKBR3, colon carcinoma RKO, osteosarcoma MG-63	(62)
Cyanobium sp. LEGE 07175		Anticancer activity		Cancer cell lines	(3)

Continuation Table 2 Bioactivities described to picocyanobacteria.

Genera	Origin	Bioactivity	Assay	Model tested	References
Cyanobium sp. LEGE 07186	Portuguese Coast	Anticancer activity	MTT and LDH	Cancer cell lines	(3)
Cyanobium sp. LEGE 06137					
Cyanobium sp. LEGE 06097					
Cyanobium sp. LEGE 06139					
Synechocystis salina LEGE 06099					
Synechocystis salina LEGE 06155					
Synechocystis salina LEGE 07173					
Synechococcus nidulans LEGE07171					
Synechococcus sp. LEGE 07172					
Synechococcus sp. LEGE 06005					
Synechococcus sp. LEGE 06026					

In a recent study of cyanobacteria isolated from the Portuguese coast, twenty eight strains were tested in eight cancer cell lines, which were selected as representative of various human tumours. From this panel of marine cyanobacteria 15 strains belong to the picocyanobacteria genera *Cyanobium*, *Synechocystis* and *Synechococcus* (3) and demonstrated potential anticancer activities by the MTT cytotoxicity assay.

Some strains belonging to the genera *Cyanobium*, *Synechocystis*, *Synechococcus* and *Leptolyngbya* were shown to have a potential source of bioactive compounds based on screenings for anticancer activity (Table 1), based on screenings with mammals (63), invertebrates (64, 65), virus, bacteria and cell lines like HT-29 and RKO (52, 66).

The marine picocyanobacterium *Prochlorococcus* produces a complex group of polycyclic lantipeptides (67). The unicellular, cyanobacterium *Prochloron didemni* also produces e a varied set of secondary metabolites, including cyclic peptides and unusual fatty acids (68). The NMR-based isolation of hierridin B from the picocyanobacterium *Cyanobium* sp. LEGE 06113 was reported by Leão et al (62) which had been isolated from the Atlantic coast of Portugal. The compound had previously been isolated from the marine filamentous cyanobacterium *Phormidium ectocarpi* (SAG 60.90) strain and showed antiplasmodial activity.

A recent study of cyanobacterial genomes (69) indicated the presence of biosynthetic gene clusters, mostly of the polyketide synthetase (PKS) among picocyanobacteria genera *Cyanobium*, *Synechococcus* and *Prochlorococcus* (62), which could be involved in the pathways leading to the production of bioactive compounds.

Although most of the research work present in the literature with a focus on bioactive compounds from marine picopcyanobacteria are performed with extracts only, the results point to picocyanobacteria of the genera *Cyanobium*, *Synechocystis*, *Synechococcus* as potentially interesting in the field of natural products.

2. Cancer

Cancer always represented for the scientific community the research area of great interest due to the high mortality rate that occurs worldwide and need to search for new treatments (70). The emergence of a cancer involves high damage to the patient health because the treatment itself used, radiation and chemotherapy, as appropriate, ultimately cause secondary damage throughout the body, to decrease the patient quality of life (71). As a result of various causes that may lead to the development of a cancer, this can affect various areas of the body, resulting in an enormous variety of cancers that affect humans today. Among the various types of cancer, based on the number of cases and deaths worldwide lung cancer, breast cancer, colorectal cancer, liver cancer and stomach cancer are the most prevalent ones (72, 73).

It is important, through the high impact that this concept presents to society, to understand how cancer form and how proliferates. One of the first studies on cancer cell metabolism goes back to the 50s of the twentieth century, when Otto Warburg showed that these cells consumed high amounts of glucose, producing high levels of lactate, even under aerobic conditions, the so-called effect of Warburg (74). The normal use of our organism cells to obtain energy, i.e., ATP, mitochondrial oxidative phosphorylation level with superior energy efficiency to lactic fermentation, used by the cancer cells. However, the use of this power generation process is extremely fast (75). Additionally cancer cells exhibit, in some cases, mitochondrial dysfunction level even with mitochondrial ATP production in considerable quantity level (76). Thus, a change in the cancer cells translates into changes in mitochondrial metabolism, with the expression changes of these organelles major components (77).

There are mechanisms that can be seen as markers of tumour progression, including: 1) high capacity of resistance to the apoptosis process with replication ability to almost endless manner and without any control the cell cycle level; 2) induction of the angiogenesis process; 3) invading other parts of the body (metastasis) (78, 79).

Chapter II – Objectives

II. Objectives

Marine cyanobacteria are well known as a source of bioactive compounds with anticancer potential. We aim with this work to characterize the toxicological properties of the marine cyanobacteria (*Synechocystis salina* LEGE 06099) compound E13010 F 5.4 by investigating the biochemical and molecular events underlying the bioactivity detected in human cancer cells, specifically in colon carcinoma (RKO) and colorectal adenocarcinoma (HT-29). The compound E13010 F 5.4 is still under structural characterization but it is already know to be a glycolipid. The specific objects of the work were the following:

1. To perform cytotoxicity assays with a selection of cancer cell lines (RKO, HT-29, MG-63, and T47D) in a concentration range of the compound E13010 F 5.4 (30 µg/mL, 3 µg/mL, 0.3 µg/mL and 0.003 µg/mL);
2. To analyze the mRNA expression of genes involved in the cell cycle (CCNB1, CCNE and P21CIP), in apoptosis (BCL-2 and BAD) and others processes (VDAC and SHMT2) by Real Time PCR;
3. To perform a non-target approach based on proteomics by two-dimensional gel electrophoresis (2DGE) and identification of differentially expressed spots by matrix-assisted laser desorption ionization time-of-flight/time-of-flight (MALDI-TOF/TOF), in order to get new insights into the mode of action of the compound.

Chapter III – Material and Methods

III. Material and Methods

1. Cyanobacterial Strain and Culture

In this work the strain *Synechocystis salina* LEGE 06099 was selected according to previous results (80). From this strain the compound E13010 F 5.4 was found to induce cytotoxicity to the cancer cell lines RKO (colon carcinoma) and HT-29 (colorectal adenocarcinoma). This strain is part of the cyanobacteria culture collection of the Laboratory of Ecotoxicology, Genomics and Evolution (LEGE) at the Interdisciplinary Center of Marine and Environmental Research (CIIMAR). For this work the culture of this cyanobacteria was mandatory in order to obtain biomass for the isolation of the compound. The compound is still under structural characterization but it is already known that is a glycolipid.

The cyanobacteria strain was cultured in large scale in Z8 medium supplemented with 20 g/L, at a temperature of 21 ˚C, brightness of 25 μmol m^{-2} s^{-1}, a photoperiod of 14h/10h (day/night) and with constant aeration, being the air filtered through a 0.2 μm filter (Sterile Syringe Filter w/ 0.2 μm Cellulose Acetate Membrane – VWR International) to prevent contamination (Figure 1).

In exponential phase the biomass was concentrated by centrifugation at 4600 rpm for 10 minutes at 4˚C. The concentrated biomass was washed twice with distilled water to remove sodium chloride, centrifuged again and stored at -20 °C. All biomass was lyophilized, weighed and stored at -20 °C until used.

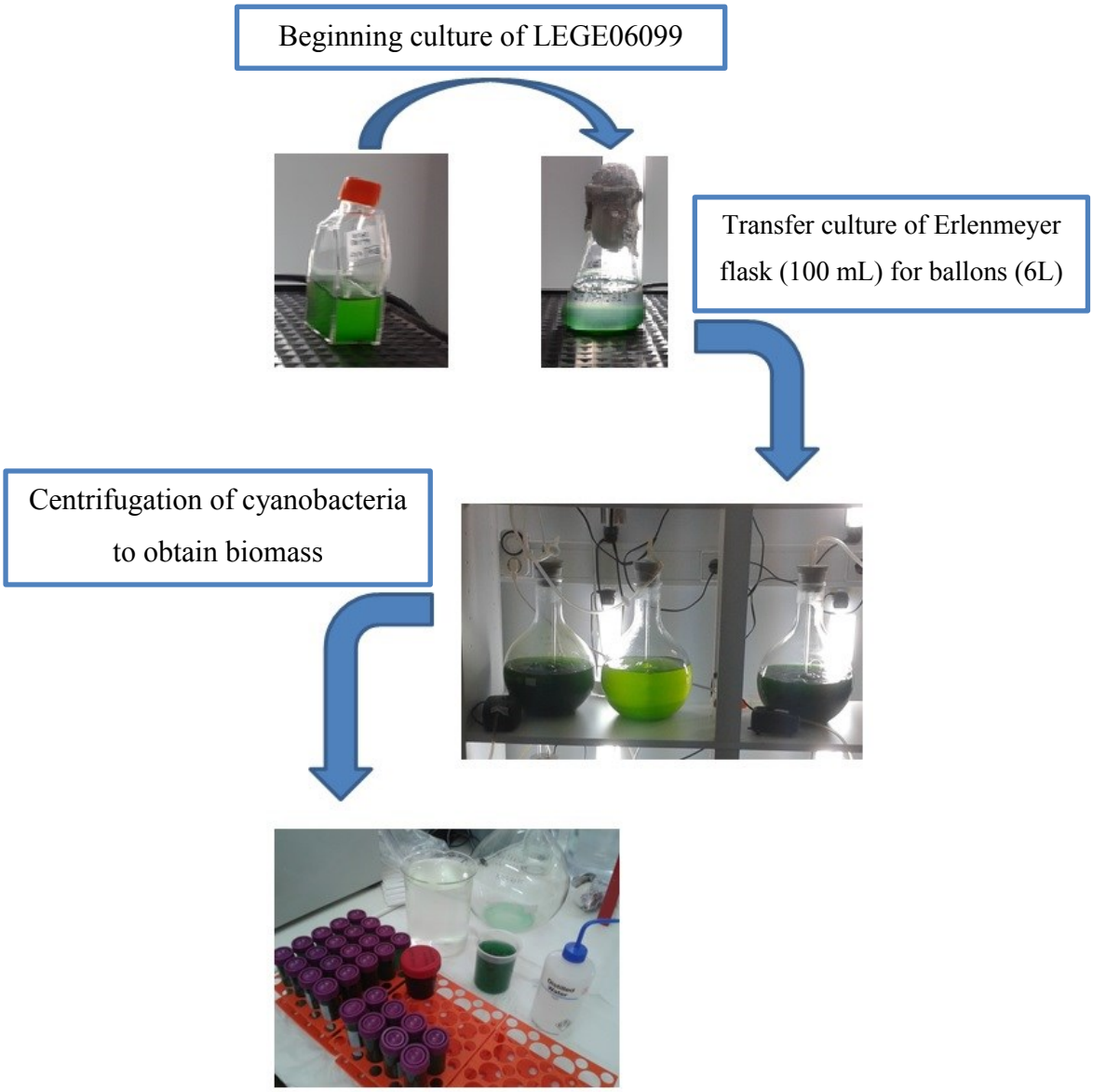

Figure 1 Process for obtaining biomass of LEGE06099.

2. Cyanobacterial Fractioning to pure compound

The extract procedure and fractionation to obtain the pure compound was the same described by Afonso, 2014 (80). A cyanobacterial crude extracts was prepared with the lyophilized material by employing an apparatus assembled as shown in Figure 2. The biomass (28.3 g) was extracted with a mixture of dichloromethane:methanol (DCM:MeOH) (2:1, v/v) (40 mL per gram of biomass). This mixture was allowed to remain for 10 minutes at room temperature, while stirring and homogenizing with a spatula. Following, the vacuum was turned on as the solvent contents were poured into the Büchner funnel and the resulting liquid phase was collected in a round bottom (RB) flask. Before starting a new step in the extraction, the biomass that had been poured was retained in a cheese cloth and recovered for a new extraction. This process was repeated two more times under these conditions and then seven times at approximately 40ºC with the use of a hotplate, for 20 minutes each, with constant stirring. Following extraction the solvents were removed in a rotary evaporator. The content of the RB flask was then resuspended and transferred to a pre-weighed glass vial, which was dried in a rotary evaporator. An amount of 3.9679 g of crude extract was obtained.

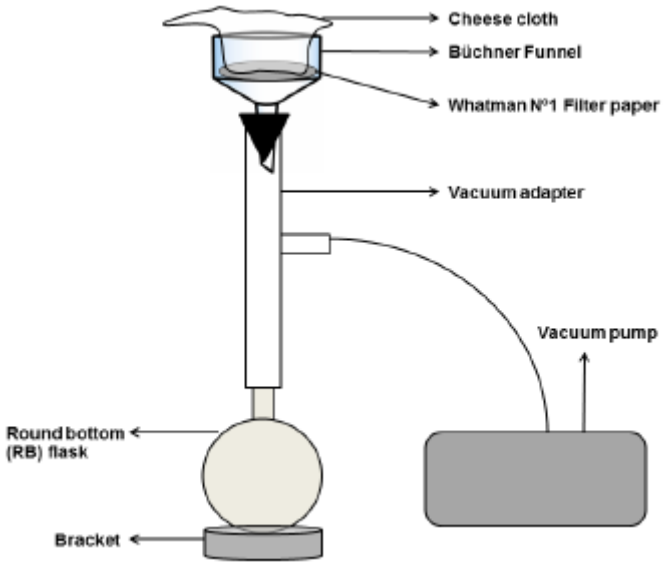

Figure 2 System assemblage for organic extraction.

The crude extract was then subjected to normal phase (silica gel 60, 0.0015-0.040 mm, Merck, KgaA, Damstadt, Germany) vacuum liquid chromatography (VLC) (Figure 3). A gradient of solvents from 9:1 hexane:ethyl acetate (Hex:EtOAc) to 100% EtOAc to 100% MeOH was used in this VLC (Table 3), so as to obtain fractions with increased polarity.

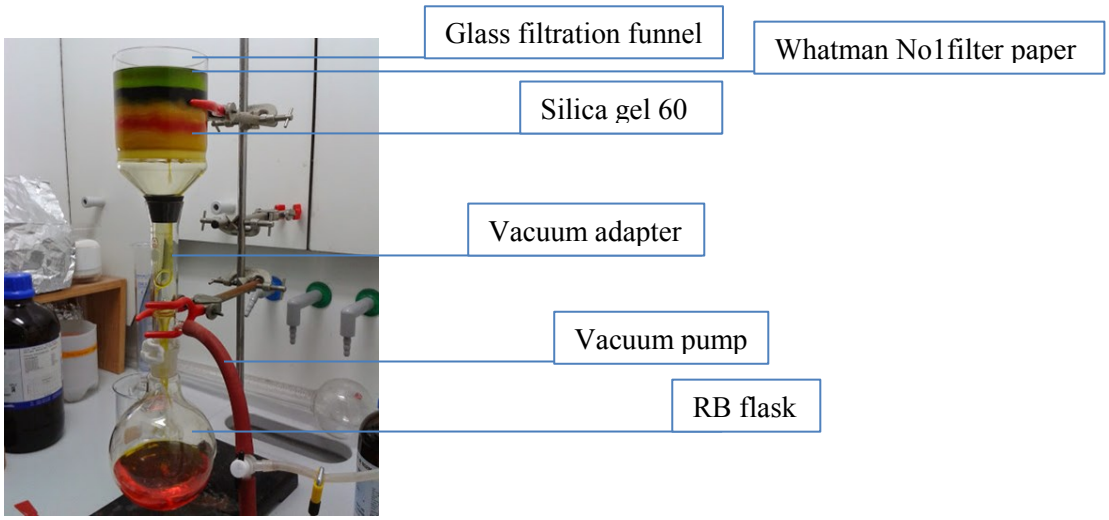

Figure 3 Apparatus for the vacuum liquid chromatography (VLC).

The crude extract was dissolved in 10% EtOAc in Hexane with help of ultrasounds and loaded onto Whatman No1 filter paper placed on top of the silica column and the solvent mixtures were added stepwise, according to Table 3, without allowing the silica surface to become dry and resulting in ten fractions A, B, C, D, E, F, G, H, Hx and I. Silica on the SI chromatography column was activated with 10% EtOAc in Hexane. The crude extract was placed in the column, followed by hexane, which was collected in an Erlenmeyer flask, until a yellow coloration reached ¾ of the column.

Table 3 Solvents volumes added to obtain 10 fractions.

Fraction	Mixture of solvents	Hex	EtOAc	MeOH	Total
A	10% EtoAc + 90% Hex	450 mL	50 mL	0 mL	500 mL
B	20% EtoAc + 80% Hex	200 mL	50 mL	0 mL	250 mL
C	40% EtoAc + 60% Hex	150 mL	100 mL	0 mL	250 mL
D	50% EtoAc + 50% Hex	125 mL	125 mL	0 mL	250 mL
E	60% EtoAc + 40% Hex	100 mL	150 mL	0 mL	250 mL
F	80% EtoAc + 20% Hex	50 mL	200 mL	0 mL	250 mL
G	100% EtoAc	0 mL	250 mL	0 mL	250 mL
H	25% MeOH + 75% EtoAc	0 mL	187,5 mL	62,5 mL	250 mL
HX	25% MeOH + 75% EtoAc	0 mL	187,5 mL	62,5 mL	250 mL
I	100 % MeOH	0 mL	0 mL	250 mL	250 mL

All the solvents in the fractions were evaporated in the rotary evaporator, and the sediment resuspended with the less volume possible of chloroform. This mixture was then transferred to 16 mL glass vials previously marked and weighted, evaporated with N_2 stream drying apparatus and stored at -20 ˚C.

After the fractioning Nuclear Magnetic Resonance spectroscopy (NMR) and Thin Layer Chromatography (TLC) were performed.

2.1. Nuclear Magnetic Resonance spectroscopy (NMR)

The NMR analysis was used to confirm the presence of the compound in the fractions. The samples were prepared in a thin-walled glass tube *Norell Standard Series™ 5mm tubes* (Sigma-Aldrich) with deuterochloroform ($CDCl_3$) (Sigma-Aldrich). NMR was performed in *Centro de Materiais da Universidade do Porto* (*CEMUP*)**.**

2.2. Sub-fractionation of Fraction F

After knowing that the compound of interest is located in the Fraction F a Sub-fractionation of this fraction was performed as shown in Figure 4.

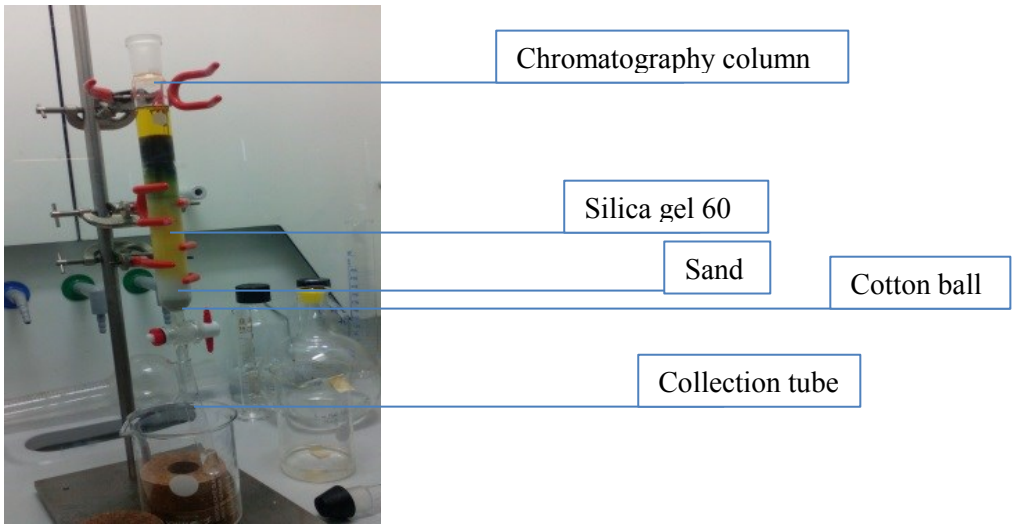

Figure 4 System assemblage for the normal phase column chromatography of fraction F.

The fraction F was dissolved in a mixture of 30% EtoAc in hex and placed on top of the silica column. A gradient of solvent mixtures was applied on the silica column with increasing in polarity, to better separate the compounds (Table 4). This chromatography was performed by gravity, 75 fractions were collected and analysed by TLC.

Table 4 Gradient used for the normal phase gravity column chromatography of fraction F.

Collection tubes	EtOAc	Hex	MeOH	Total Volume
1 – 4	30%	70%	-	250 mL
5	40%	60%	-	100 mL
6	40%	60%	-	100 mL
7 – 8	40%	60%	-	100 mL
9 – 24	40%	20%	-	500 mL
25 – 30	40%	-	-	250 mL
31 – 34	80%	-	-	250 mL
35 – 41	100%	-	-	250 mL
42 – 52	75%	-	25%	500 mL
53 – 63	75%	-	25%	250 mL
63 – 75	75%	-	25%	250 mL

2.3. Thin Layer Chromatography (TLC)

For TLC 10 µL of samples in were placed in *TLC silica gel 60 F254* plates. Plates were placed in a tank mixture of solvents, EtOAc in Hex (50:50), observed in the UVs (366 nm absorbance) and the areas to be marked up the compounds of interest. The silica plates were immersed in the acid phosphomolybdic acid (PMA DIP) and put on a hotplate until they see the compounds.

2.4. HPLC for the isolation of the compound

The isolation of the compound was performed in HPLC following the protocol described in Afonso, 2014. This step was not performed during this thesis.

3. Cell Culture and Cytotoxicity Assays

Cytotoxic assays were firstly performed with the human colon adenocarcinoma cell line HT-29 and RKO, the osteosarcoma cell line MG-63 and the breast carcinoma cell line T47D in order to infer about selective toxicity. HT-29 and T47D cells were purchased from Sigma-Aldrich; MG-63 and RKO cells were obtained from the American Type Culture Collection (ATCC). The selection of this cancer cell lines was based in previous results of cytotoxicity of the compound in different cell lines (3).

Cells were cultured in DMEM GlutaMAX medium (Dulbecco's Modified Eagle Medium DMEM GlutaMAX^{TM} – Gibco – Invitrogen), supplemented with 10% (v/v) Fetal Bovine Serum (Gibco – Invitrogen), 1% Fungizone (Gibco – Invitrogen) and 1% Penicillin-Streptomycin (Pen-Strep 100 IU/mL and 10 mg/mL, respectively) (Gibco – Invitrogen). Cells were maintained in a humidified incubator at 37 ˚C, with 5% CO_2.

The cytotoxicity of the compound was assessed by the reduction in cell viability measured by the reduction of 3-(4.5-dimethylthiazol-2-yl)-2.5-diphenyltetrazolium bromide (MTT), a yellow tetrazole soluble in water, to purple formazan crystals. The reduction of MTT to formazan is directly proportional to the mitochondrial activity and consequently cell viability.

Cytotoxicity assays were performed in 96-well plates. All cell lines were seeded at $3.3x10^4$ cel/mL. After 24h of adhesion, cells were exposed to new medium with the compound a

range of concentrations of 30 µg/mL, 3 µg/mL, 0.3 µg/mL, 0.03 µg/mL and 0.003 µg/mL for 24 and 48 hours. After treatment cells were incubated with 0.05 mg/mL MTT for 3 hours. At the end of this period, the medium was aspirated and the formazan crystals dissolved in 500 µL 100% DMSO (Panreac). The absorbance was read at 550 nm in a *Gen 5™ – Multi – detection Microplate Reader* (Biotek).

From this assays the cancer cell lines RKO and HT-29 were selected to perform genomic and proteomic assays.

3.1. Exposure to cyanobacterial compound E13010 F 5.4 for genomics and proteomics

RKO and HT-29 cells were cultured in 24-well plates (Orange Scientific) at a density $1x10^6$ cells/mL. After 24 hours of culture, the medium was removed and was replaced by medium supplemented with: 1) 20% DMSO (negative control group); 2) 1% DMSO (positive control group) and 3) cyanobacteria compound a range of concentrations of 30 µg/mL; 3 µg/mL; 0.3 µg/mL; 0.03 µg/mL; 0.003 µg/mL. Initially all these concentrations were tested in order to select an exposure concentration for the genomics and proteomics analyses. Finally, the 30 µg/mL concentration was selected. In all assays 6 replicates were performed. In parallel to the exposure of cells for proteomics and genomics, cells were exposed to the compound for MTT, using 3 replicates for treatments and controls, in order to certificate its cytotoxicity.

To collect cells after exposure to the compound E13010 F 5.4, the medium was aspirated and cells were washed with PBS (250 µL per well). Cells were then trypsinized (0.25% Trypsin-EDTA, Gibco – Invitrogen) (200 µL per well) transferred to an 1.5 mL Eppendorf tube, centrifuged at 1200 rpm for 5 minutes and stored as cell pellet at -80 °C for posterior analysis.

4. Gene Expression Analysis

4.1. RNA isolation and cDNA synthesis

Total RNA was extracted from the cells exposed to compound and negative control to investigate the expression of the mRNA. To do this, we used *Total RNA Isolation* (Macherey-Nagel) kit and chosen protocol was *Total RNA purification from cultured cells, laser captured cells, or microdissected cryosections with Nucleospin® RNA XS*. The protocol is based on 10 stages: 1 – supply samples (provide sample such as a pellet of up to 5 x 10^5 cells); 2 – lyse and homogenize cells; 3 – add Carrier RNA (it step was not performed); 4 – filtrate lysate; 5 – adjust RNA binding condition; 6 – bind RNA; 7 – desalt silica membrane; 8 – digest DNA; 9 – wash and dry silica membrane; 10 – elute highly pure RNA (used 30 µL of water RNase-free).

After this process, RNA was quantified with the *Qubit® Fluorometer* (Invitrogen), using two standards and following the manufacturer instructions.

The quality of the extracted RNA was accessed by 1% agarose gel electrophoresis. RNA quality was considered good, if the bands were sharp, with the 28S band being about twice as intense as the 18S band.

Transcription of RNA into cDNA was performed by reverse transcription (RT) using the *iScript™ Reverse Transcription Supermix for RT-qPCR* (Bio-Rad) using oligo (dT) primer. 1 µg of total RNA was reverse-transcribed in a 20 µL reaction; 4 µL 5x iScript reverse transcription supermix; RNA template ($\frac{1000\,ng\,x\,1\,\mu L}{concentration\,of\,sample\,\mu g/mL}$); nuclease-free water (RNA template – 13 µL). Samples of cDNA were stored at -20˚C.

4.2. Evaluation of Primer

The cDNA products were used for analysis of primer performance of a set of selected human genes (RPL8, HPRT1, VDAC, SHMT2, CCNE, CCNB1, P21CIP, BCL-2, BAD) (Table 5). For performance evaluation in real-time PCR in the conditions given in the next paragraph, standard curves were analysed from the diluted cDNA pool. The resulting amplification efficiency of the primers should be between 86.4% and 108.2%. The view of the melt curve from the RT-PCR analysis monitored the specificity of the performed reaction.

Primers were previously ready and evaluation had been made in a previous work (81).

Table 5 Selected primers main information in *NCBI* (82).

Name	Function	Primer sequence	Efficiency	Annealing temperature
RPL8 (Ribosomal protein L8)	Encodes a ribosomal protein that is a part of the 60S subunit.	Forward: 5'GTGTGGTG GCTGGAGGT G3' Reverse: 3'CGATGTGC TGGTGGTTGC 5'	101,4%	57 ˚C
HPRT1 (Hypoxanthine Phosphoribosy l transferase)	Converts hypoxanthine to insonie monophosphate and guanine to guanosine monophosphate. Central role on generating purine nucleotides.	Forward: 5'TGGCGTCG TGATTAGTGA TG3' Reverse: 3'CAGAGGGC TACAATGTG ATGG5'	96,5%	57 ˚C
VDAC (Voltage-dependent anion channel)	Encodes a voltage-dependent anion channel protein that is a major component of the outer mitochondrial membrane.	Forward: 5'CGGAAGGC AGAAGATGG C3' Reverse: 5'TTGGTGGT CTCAGTGTTG G 3'	94,6%	57 ˚C
SHMT2 (Serine hydroxymethy transferase 2)	Encodes the mitochondrial form of a pyridoxal phosphate-dependent enzyme that catalyzes the reversible reaction of serine and tetrahydrofolate to glycine and 5, 10-methylene tetrahydrofolate, which is responsible for glycine synthesis.	Forward: 5'CTGCGACTTC CGAGTTGCGATG 3' Reverse: 5'GGCTGCGTTG CTGTGCTGAG3'	95,1%	57 ˚C
CCNE (Cyclin E1)	Regulates the subunit of CDK2, required for the cell cycle G1/S transition.	Forward: 5'GTTCTCGG CTCGCTCCAG 3'	86,4%	57 ˚C

		Reverse: 3'CGGTCATC ATCTTCTTTG TCAGG5'		
CCNB1 (Cyclin B1)	Essential for the cell cycle control at G2/M (mitosis) transition.	Forward: 5'CTAAGATT GGAGAGGTT GATGTC3' Reverse: 3'CAGGTAAT GTTGTAGAGT TGGTG5'	91%	57 ˚C
P21CIP (Cyclin-Dependent Kinase Inhibitor 1A)	Binds and inhibits cyclin-dependent kinase activity and blocking cell cycle progression.	Forward: 5'GGGACAGC AGAGGAAGA C3' Reverse: 3'CGGCGTTT GGAGTGGTA G5'	96%	55 ˚C
BCL-2 (B-Cell CLL/ Lymphoma)	Acts as anti-apoptotic regulators that are involved in a variety of cell activities. The proteins encoded reduce the release of pro-apoptotic cytochrome c from mitochondrial and block caspase activations. Have two transcripts: alpha and beta. (We used the alpha transcript.)	Forward: 5'GTGTGGAG AGCGTCAAC C3' Reverse: 5'CTTCAGAG ACAGCCAGG AG3'	108,2%	55 ˚C
BAD (BCL2-Associated Agonist Of Cell Death)	Regulates cell apoptosis, forming heterodimers with BCL-xL and BCL-2 and reversing their death repressor activity.	Forward: 5'GAGGATGA GTGACGAGT TTGTG3' Reverse: 5'CGGGATGT GGAGCGAAG G3'	107,1%	59˚C

4.3. Real-Time PCR

For the study on mRNA expression, a Real-Time PCR using the *iQ5 Multicolor Real-Time PCR Detection System* (Bio-Rad) was performed in a final reaction volume of 20 µL with 10 µL iQ supermix, 0.4 µL forward and reverse primer (given the final concentration of

200 nM each), 1 µL 1x iQ SYBR Green Supermix (Bio-Rad), 2 µL cDNA sample (1:10 diluted) and 7.2 µL sterile water. The samples were run with a duplicate negative control (NTC) to assure the absence of contaminations, and with a duplicate of standard cDNA pool from RKO cells without treatment (1:10 diluted).

Standard curves were analysed from the diluted cDNA pool and the resulting amplification efficiency of the primers should be between 86.4% and 108.2%. The view of the melt curve from the RT-PCR analysis monitored the specificity of the performed reaction.

For the correct RT-PCR mRNA expression in the *Bio-Rad iQ5* software, the step point should be on the "annealing temperature" of each gene, the analysis mode is "PCR base line subtracted" and the baseline threshold was selected at the value of 80.

To perform the gene normalization in a previous work (81) was used the *NormFinder* software. With the results obtained was selected genes RPL8 and HPRT1.

5. Proteomic Analysis

The proteomic analysis was performed with the purpose of knowing the main differences in protein expression regarding the effect of cyanobacterial fraction in the selected cell line.

5.1. Protein extraction from cells after exposure to the compound E13010 F 5.4 and quantification

The protein extraction was performed by adding to the cell pellet a volume of solubilisation buffer (SB – Table 6) at a ratio of 80 µL to 15 mg of cell biomass. The cell line RKO proteins were extracted 2x on vortexing, each 30 seconds followed by sonication and cell line HT-29 were extracted 2x on vortexing, each 30 seconds. The homogenization process took 1 hour in the ice for RKO and 30 minutes for HT-29 and then the homogenate was centrifuged at 16,000 g, for 20 minutes, at 4 ˚C. The supernatant was collected and proteins were quantified using the Bradford method (Bradford, 1976). The protein samples were stored at -80 ˚C.

Table 6 Solubilisation buffer.

Urea (7 M)	4.2 g
Thiourea (2 M)	1.52 g
CHAPS (4%, w/v)	0.4 g
Dithiothreitol (DTT) (65 mM)	0.1 g
Ampholytes (0.8%, v/v, pH 4-7)	8 µL
Ultra-pure water	2 mL
TOTAL VOLUME	10 L

5.2. Two-dimensional Electrophoresis (2DGE)

The proteins were separated by two-dimensional electrophoresis (2DGE) that separates proteins by their isoelectric point and molecular weight. Protein samples in the final concentrations indicated in Appendix 6, Table 19 were diluted in 125 µL of solubilisation buffer (SB) with 1 µg bromophenol blue (BPB) and centrifuged at 10 rcf for 10 minutes. Then, the protein samples were loaded in 11 cm, pH 3-10 IEF gel strips (Bio-Rad) being part of the acrylamide gel contact with the sample, applying 3 mL of mineral oil on top of the strip. The support was then transferred to the voltmeter (Bio-Rad Protean IEF Cell) and proteins separated by isoelectric focusing (IEF) with the following program:

- Gel rehydration 12 hours at 50 V;
- **Step 1** – 250 V for 15 minutes;
- **Step 2** – 2 hours voltage gradient to 4000 V (linear ramp);
- **Step 3** – 4000 V until achieving 20000 V/h (linear ramp).

At the end of the first dimension, the IEF gel strips were stored at -20 ˚C until performing the second dimension, SDS-PAGE. Before the second dimension electrophoresis IEF gel strips need to be equilibrated using two solutions (Table 7), Equilibration Buffer 1 with 12.5 mg/mL dithiothreitol (DTT) and Equilibration Buffer 2 with 25 mg/mL iodoacetamide in urea (6 M), glycerol (30%, v/v), SDS (2%, w/v), both during 15 minutes with slow agitation and with 2 mL of each solution to an IEF strip.

Table 7 Equilibration Solution (EqS).

Tris-HCl (1,5 M, pH 8,8 stock solution)	10 mL
Urea (6 M)	72.1 g
Glycerol (29.3 %, v/v)	69 mL
SDS (2%, w/v)	4 g
Bromophenol blue	4 mg
TOTAL VOLUME	200 mL (with H_2O)
Equilibration buffer 1	Add 100 mg DTT to 10 mL of EqS
Equilibration buffer 2	Add 250 mg of iodoacetamide to 10 mL EqS

The second dimension consisted of polyacrylamide gel electrophoresis 12.5% (w/v) under denaturing conditions (SDS-PAGE). Electrophoresis was performed in the power supply system *Hoefer PS600* coupled vertical unit electrophoresis *SE900* (Hoefer, EUA, Massachusetts). The electrophoresis system enables the six gels run at the same time. For the polymerisation were required a volume of 400 mL. Gels were prepared as follows: 166.7 mL acrylamide 30% (w/v) (Bio-Rad, USA, California); 124,8 mL destilled water; 100 mL gel buffer (1,5 M Tris-HCl, pH 8,8); 4 mL 10% SDS (Sodium Dodecyl Sulfate) (Sigma-Aldrich); 4mL 10 % APS (Ammonium Persulphate) (Sigma-Aldrich) and 0.55 mL 10% TEMED (N, N, N', N' - tetramethylehylendiamine) (Bio-Rad). After equilibration of isoelectric focusing, strips were applied on these gels alongside molecular weight molecular markers (Bio-Rad). Electrophoresis of the second dimension was done with constant amperage of 480 mA for a period about 6 hours.

5.3. Fixation and staining of polyacrylamide gels

After the electrophoresis run, each of the polyacrylamide gels were fixed for 24h using a mixture of 2 L distilled water, 800 mL methanol (40%, v/v) (Merck, USA, New Jersey) and 200 mL acetic acid (10%, v/v) (Panreac, Spain, Barcelona), using 200 mL per gel.

Gels were stained according to the protocol described in the article of Neuhoff V. (75). For Coomassie Blue staining 4 volumes of the staining solution were mixed with 1 volume of methanol, with constant agitation using 200 mL each gel. Solution A is made up of 10 mL ortho-phosphoric acid (2%, w/v) (Merck), 50 g ammonium sulphate (10% w/v) (Fisher Scientific, USA, Massachusetts) and 500 mL distilled water. Solution B contains 0.5 g Coomassie Blue G250 (5%, w/v) (Sigma-Aldrich) and 10 mL distilled water. Before

application of the staining mixture, each gel was washed with 100 mL of mili Q water during 10 minutes. Each gel was then stained under constant agitation overnight. In the end of the staining procedure, gels were extensively washed with mili Q water to remove the colloidal particles, 5x for 10 minutes, until the water stays transparent and is not blue anymore, and stored in the storage solution with 400 g ammonium sulphate (20%, w/v) (Fisher Scientific, USA, Massachusetts) and 2 L of distilled water at room temperature.

5.4. Gel Image Acquisition and Protein Expression Analysis

Digital image from the gels were obtaining using the software *Quantity One* (Bio-Rad) associated with the densitometer *GS-800* (Bio-Rad), reproducing the sensitivity parameters for all the gel images. The images obtained were analysed for differentially expressed spots using software *PDQuest Advanced 8.0* (Bio-Rad) and consisted of: detect spots on the gels; align gels; determine the relative intensity of each spot. The spot detection and matching was manually revised in the software. When the protein expression was analysed, a master gel was created in the software, which contained all the spots detected in the 2DGE gel images. Software analysis allowed us to make quantitative and qualitative comparisons of spots between gels, calculate values of molecular weight and isoelectric points. The spot expression (presence/absence) and intensity variations were also analysed, by comparing each protein spot between all the gels in the experimental groups. The quantitative variations were statistically evaluated by the t-student and Mann-Whitney tests ($p \leq 0.05$). This screening process was done for each gel control and treatments group, and has been analysed 4 replicate gels per group. In total of 16 gels were analysed for both cell lines (8 for RKO and 8 for HT-29).

5.5. Preparation of proteins samples for matrix-assisted laser desorption/ionization (MALDI) time-of-flight / time-of-flight (TOF/TOF)

Matrix-assisted laser desorption/ionization (MALDI) time-of-flight/time-of-flight (TOF/TOF) high-resolution tandem mass spectrometer is used for protein identification. This instrument has high sensitivity for peptide analysis associated with MALDI and comprehensive fragmentation information provided by high-energy collision-induced dissociation (CID).

Subsequently the selection of spots with biological interest using the software *PDQuest Advanced 8.0* (Bio-Rad), they were excised from the gels and washed the spots with 30 µL of ultra-pure water for 20 minutes at room temperature. Thereafter, water was removed by adding 30 µL of acetonitrile (ACN) 50% and incubated for 30 minutes at room temperature with stirring, to remove all coloration of the gel pieces. After complete discoloration of the gel pieces, ACN was removed and added 30 µL ACN 100% and remained at room temperature and stirred for 5 minutes and repeat the process for 30 minutes. Afterword, the solvent was removed and the gel pieces dried overnight at room temperature. After being totally dried, was added 20 µL of trypsin at a concentration of 6.7 ng/µL for 30 minutes on ice. Removal of trypsin and added 20 µL of ammonium bicarbonate (Sigma), digestion overnight at 37 ˚C, and storage of peptides at -20 ˚C.

For application in MALDI-TOF/TOF plate, the samples were previously concentrated and desalted using micro columns 10 µL *Pierce® C18 Tips* (Thermo Scientific), using a micro column per sample. The columns were activated with 50% ACN with two cycles of 10 µL, then being equilibrated with trifluoroacetic acid (TFA) (Sigma-Aldrich), again two cycles of 10 µL. To bind the peptides to the column aspire and dispense 10 µL of the sample ten cycles. After the 10 cycles, dispense the volume sample back to the PCR tube. Wash the column with two cycles of 10 µL rinse solution (0.1% TFA in 5% ACN) and dispense to waste. Since the peptides are already bind to the column, the rinse solution should be distributed into individual PCR tubes (about 30 µL) for each sample to avoid contamination between samples. The peptides were eluted with the matrix for MALDI identification (100% ACN of 500 µL, 5% TFA of 20 µL, 7-8 mg of α-cyano-4-hydroxycinnamic acid (Sigma) of 7 mg and distilled water of 480 µL). Separate 2.5 µL of the matrix to clean PCR tubes and pipette and dispense the solution until five times. Dispense 1.7 µL of peptide solution on the MALDI plate *Opti-TOF™ 384 Well Insert* (123 x 81 mm) (Applied BioSystems) avoiding bubble formation that may affect the peptide crystallization on the plate. Final identification by MALDI-TOF/TOF was acquired as service from the IPATIMUP (Institute of Molecular Pathology and Immunology of the University of Porto), Porto.

Chapter IV – Results

IV. Results

1. Cyanobacterial Fractioning to pure compound

During eight months the cyanobacteria strain LEGE 06099 was cultured in around 100 L and was obtained 28.3 g of lyophilized biomass from which the compound was extracted. The ten fractions obtained during fractionation were analysed by Nuclear Magnetic Resonance spectroscopy (Appendix 1, Figure 19 – 27). As expected from previous work (85) the compound of interest was located in the fraction F (Figure 5), singlets at δ6:50 and δ6:35.

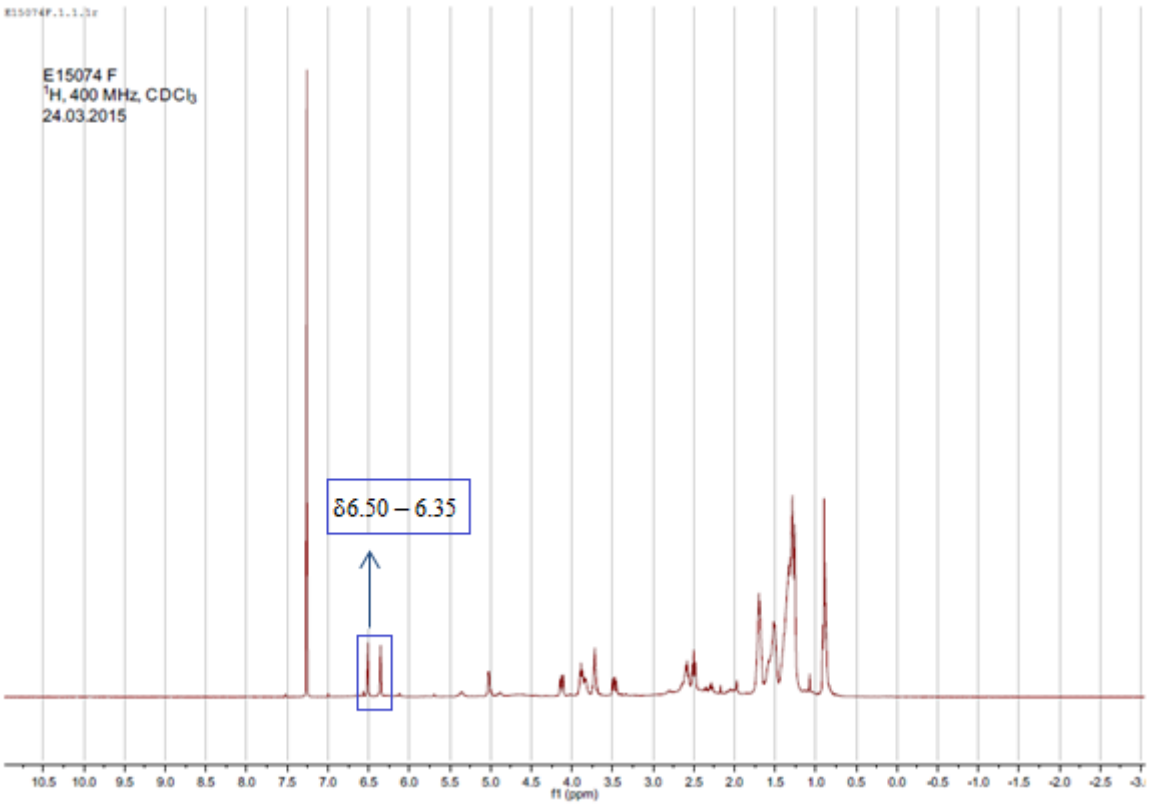

Figure 5 Fraction F.

1.1. Thin Layer Chromatography (TLC)

The 75 sub-fraction were tested on twelve TLC plates (Appendix 2, Figures 28 – 39). The individual compounds appear as spots and run different distances. The compounds are grouped as it travels over the same distance. Therefore, there was obtained seven groups, as shown in Table 8.

Table 8 Sub-fractions have been grouped.

Sub-Fraction	Group
1 – 4	---
5 – 6	1
7	2
8	3
9 – 10	4
11 – 24	5
25 – 30	6
31 – 75	7

2. Cell Culture and Cytotoxicity Assays

2.1. Exposure to cyanobacterial compound E13010 F 5.4 and cytotoxicity assays

For the evaluation of the cytotoxicity induced by the compound E13010 F 5.4 four tumour cell lines (HT-29, RKO, MG-63 and T47D) and concentration range (30 µg/mL, 3 µg/mL, 0.3 µg/mL, 0.03 µg/mL and 0.003 µg/mL) were assayed in 96-well plates, at a concentration of $3.3x10^4$ cell/mL, with two exposure times, 24 and 48 hours (Appendix 3, Figures 40 – 43), but only the tumour cell line RKO and HT-29 at a concentration 30 µg/mL was selected for the following mRNA expression and proteomic analyses.

The MTT assay is a fast colorimetric method used to measure cell proliferation and to screen for anticancer drugs. The method is based on reduction of the tetrazolium salt, MTT (3-(4,5-dimethylthiazol-2-yl)-2,5-diphenyltetrazolium bromide) by actively growing cells to purple formazan crystals, which accumulate in endosomal and/or lysosomal compartments, being later transported out of the cell by exocytosis. Due to the fact that this a fundamental mechanism of living cells, this assay has been frequently used to determine cellular viability (83). The MTT assay was used to evaluate the effect of the compound

E13010 F 5.4 on the inhibition of cellular proliferation of human tumour cell lines and cytotoxicity.

The results regarding cell viability of the RKO and HT-29 tumours cells lines exposed of the compound E13010 F 5.4 at a concentration of 30 µg/mL in 24-well plates, at a concentration of $1x10^6$ cell/mL and for 24 hours are presented in Figures 6 and 7. The negative control consisted of growth medium with 1% DMSO and a positive control 20% DMSO with growth medium. The reduction in cell viability of both tumour lines proves the cytotoxicity of the compound E13010 F 5.4. The difference in cell concentration in 24 and 96-well plates is due to the fact that did not have enough cells and therefore results in difference from the previous work (80).

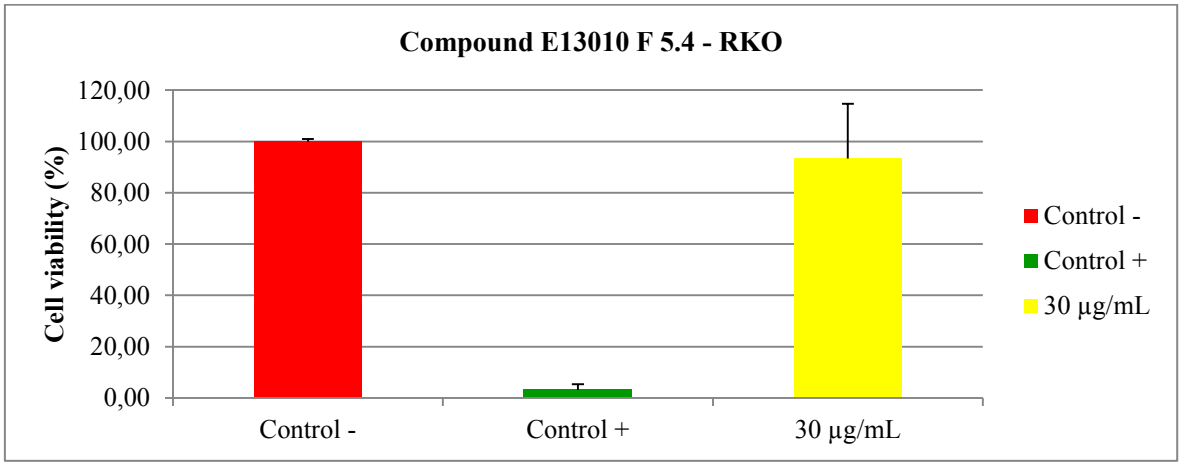

Figure 6 Cell viability from compound E13010 F 5.4 of the cyanobacterial strain LEGE06099, in the RKO tumour cell line, at a concentration 30 µg/mL, with exposure time of 24 hours at $1x10^6$ cells per well. The negative control corresponds to 1% DMSO (90 µL) and the positive control to 20% DMSO (400 µL).

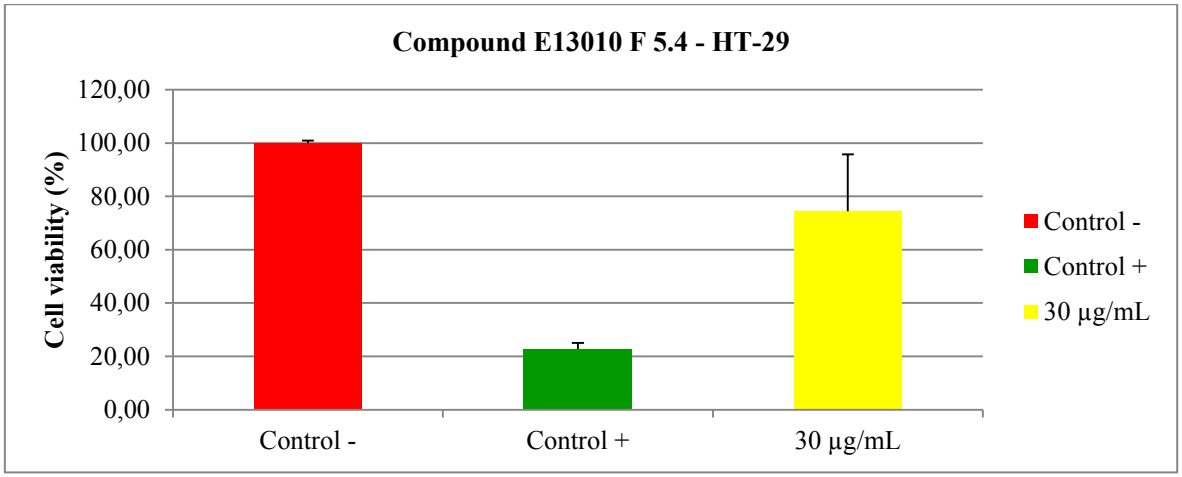

Figure 7 Cell viability from compound E13010 F 5.4 of the cyanobacterial strain LEGE06099, in the RKO tumour cell line, at a concentration 30 µg/mL, with exposure time of 24 hours at $1x10^6$ cells per well. The negative control corresponds to 1% DMSO (90 µL) and the positive control to 20% DMSO (400 µL).

3. Gene Expression Analysis

3.1. RNA isolation and cDNA

After the process with *Total RNA Isolation* (Macherey-Nagel) kit, RNA was quantified with the *Qubit® Fluorometer* (Invitrogen) (results from quantification in Appendix 4 Table 11). After quantification, the quality of RNA was confirmed with agarose gel electrophoresis as presented in Figures 8 and 9. RNA quality was considered as reasonably, since sharp bands were obtained for 28S and 18S rRNA. The absence of the 28S:18S rRNA ratio of 2:1 was observed, but regarded as uncritical since no signs of genomic contamination or RNA degradation were present.

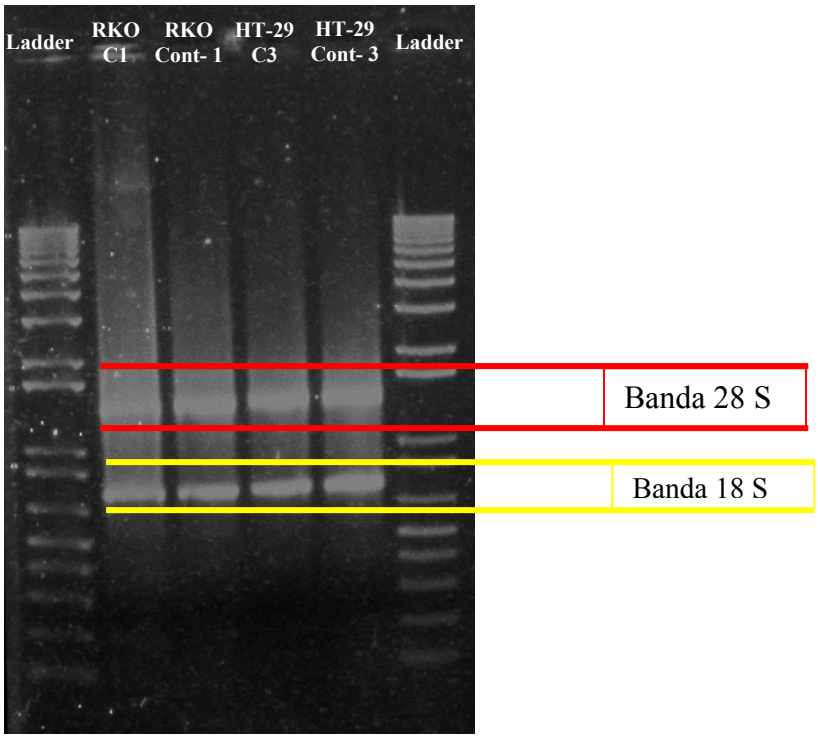

Figure 8 Agarose gel electrophoresis for the samples treated with tumour RKO cell line, replicate 1 treated with compound and replicate 1 for negative control and samples treated tumour HT-29 cell line, replicate 3 treated with compound and replicate 3 for negative control.

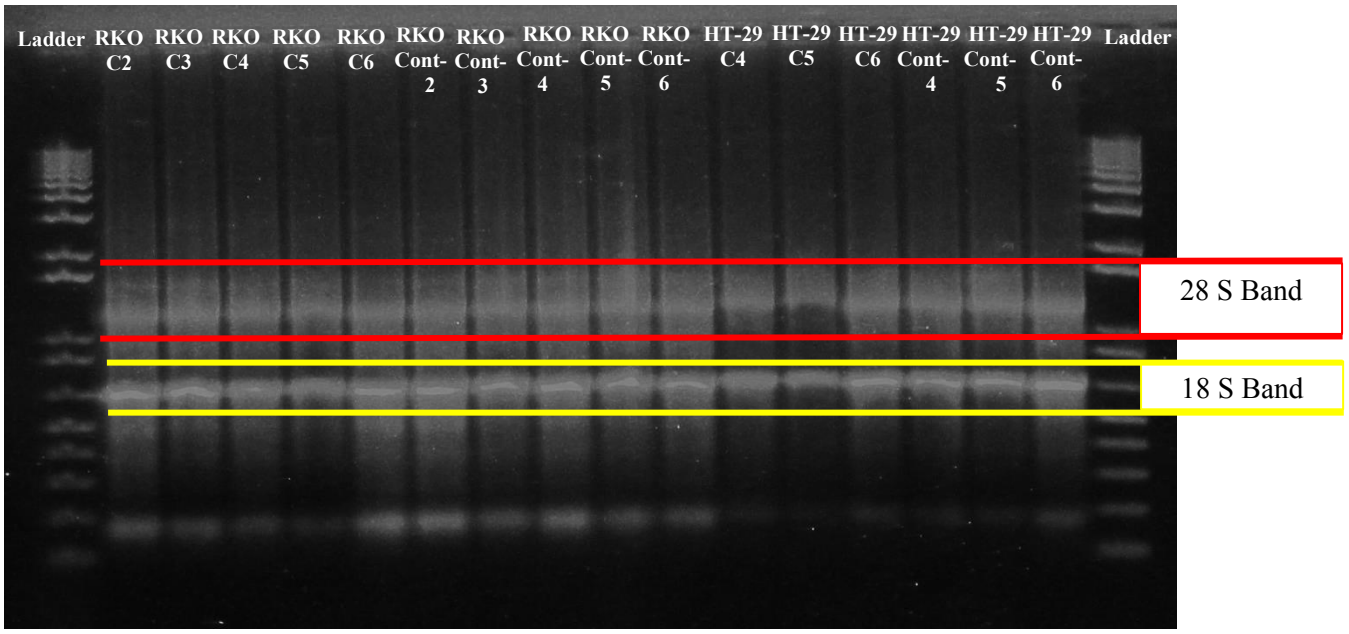

Figure 9 Agarose gel electrophoresis for the samples treated with tumour RKO cell line, replicate 2, 3, 4, 5, 6 treated with compound and replicate 2, 3, 4, 5, 6 for negative control and samples treated tumour HT-29 cell line, replicate 4, 5, 6 treated with compound and replicate 4, 5, 6 for negative control.

3.2. Real-Time PCR

Effects of the compound on cells were analysed by mRNA expression of genes involved in molecular mechanisms of the cell. The target genes selected for this analysis were RPL8, HPRT1, VDAC, SHMT2, CCNE, CCNB1, P21CIP, BCL-2 and BAD, comprising genes from the cell cycle regulation and apoptosis. The RPL8 and HPRT1 genes were used as reference genes in accordance to a previous study of our working group (81). The mRNA expression was analysed between two different groups: a control group were RKO and HT-29 cells were exposed to 1% DMSO; a treatment group where RKO and HT-29 cells were exposed to the cyanobacterial compound E13010 F 5.4. The results of Real-Time PCR are on the Appendix 5, Table 12 – 18.

After obtaining these data, we used the *GraphPad Prism*® software. The program used the Kolmogorov – Smirnov test, the Student T – test and the Mann-Whitney test. The test Kolmogorov – Smirnov can be used to evaluate two hypotheses: the data follow a normal distribution or the data does not follow a normal distribution. The Student T – test is parametric and requires a normal distribution. It is used on two independent samples. The Mann-Whitney test (Wilcoxon rank-sum test) or U – test is indicated for comparison of two unpaired groups to see if they belong or not to the same population. The U – test is

non-parametric and is used in independent random samples and testing the equality of medians. The U values evaluating the degree of entanglement of the data of the two groups after ordering. The greater separation of the data set indicates that the samples are different, rejecting the hypothesis of equality of medians.

Analysis of mRNA expression in cell cycle genes, CCNB1, CCNE and P21CIP in the RKO cell line indicated that there are no significate changes in CCNB1 and CCNE genes expression, but there are significant changes in P21CIP gene ($p < 0.05$ significant value) (Figure 10).

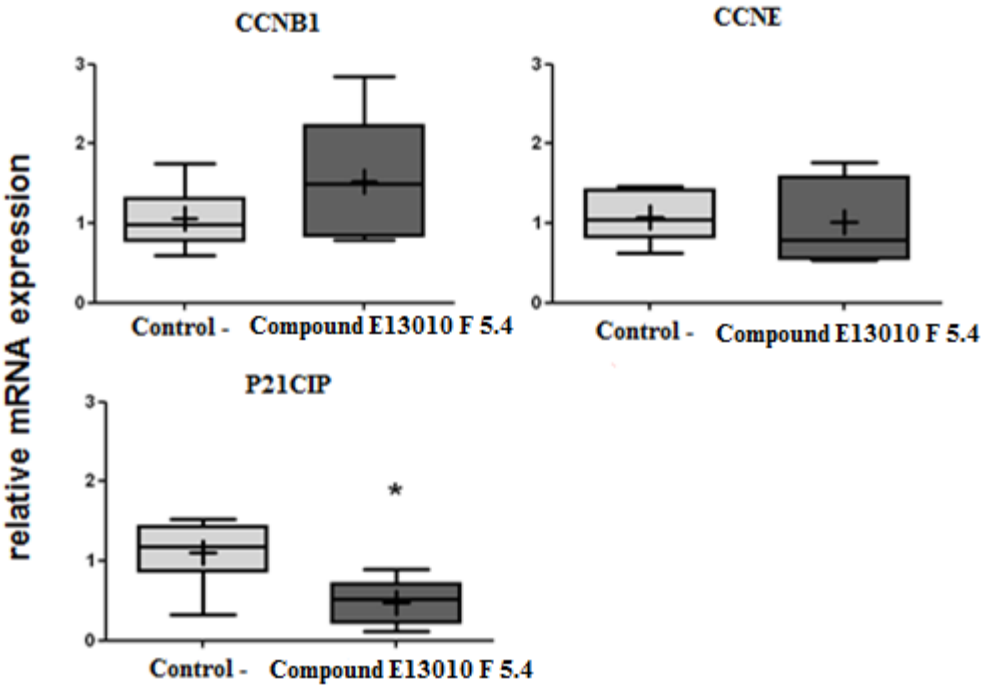

Figure 10 Relative mRNA expression from selected cell cycle genes CCNB1, CCNE, P21CIP treated with RKO cell lines (* $p < 0.05$ significant value).

In the apoptotic genes BCL-2 and BAD and also in the RKO cell line, there was only a small change in the gene BAD (p=0.087) exposed to the cyanobacterial compound (Figure11). The change does not have significant value, but indicates a tendency.

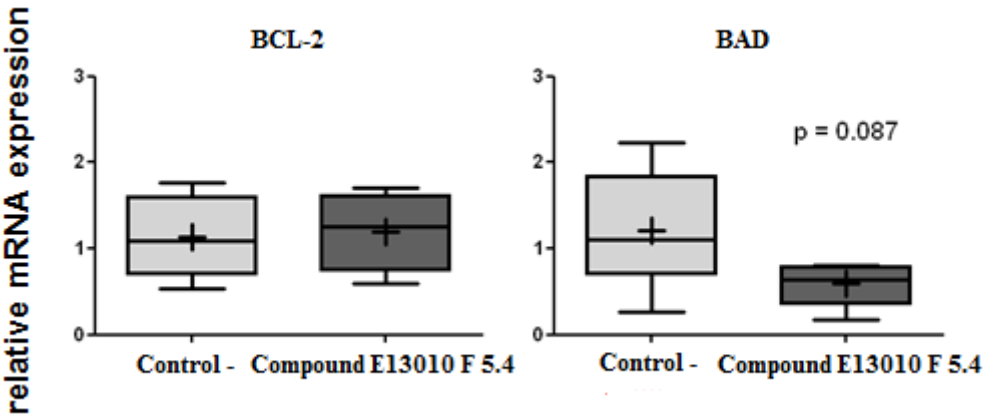

Figure 11 Relative mRNA expression from selected apoptosis genes, BCL-2 (anti-apoptotic) and BAD (pro-apoptotic) treated with RKO cell lines.

In other genes related to cancer (VDAC and SHMT2) of cell line RKO, no changes were observed between the control group and the group exposed to the cyanobacterial compound (Figure 12).

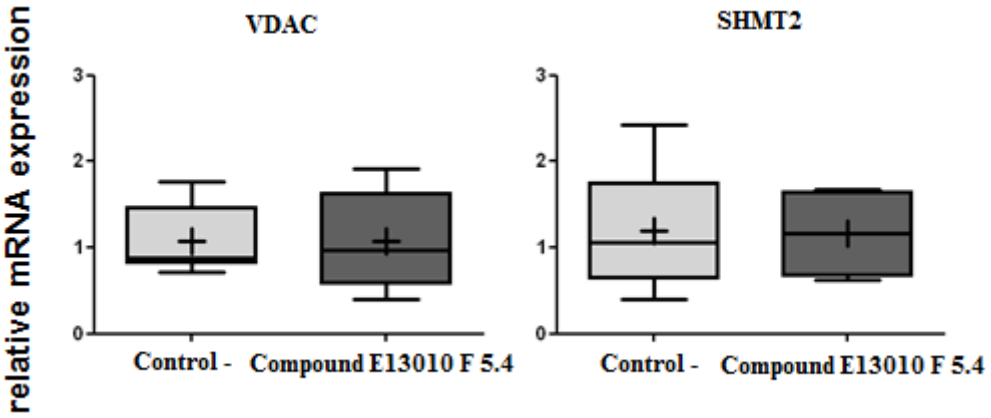

Figure 12 Relative mRNA expression from other cancer-related genes, VDAC and SHMT2 treated with RKO cell lines.

Regarding the analysis of mRNA expression of the genes of cell line HT-29, no significant changes were observed both in cell cycle genes (Figure 13), as in apoptotic genes (Figure 14). However, in other cancer-related genes, including the gene VDAC (Figure 15) mRNA expression seemed increased (p=0.114), but the value was not statistically significant. This may be due to the fact that instead of 6 replicas were used only 4 since due to low yield in protein extraction two replicates from genomics were dedicated to proteomics.

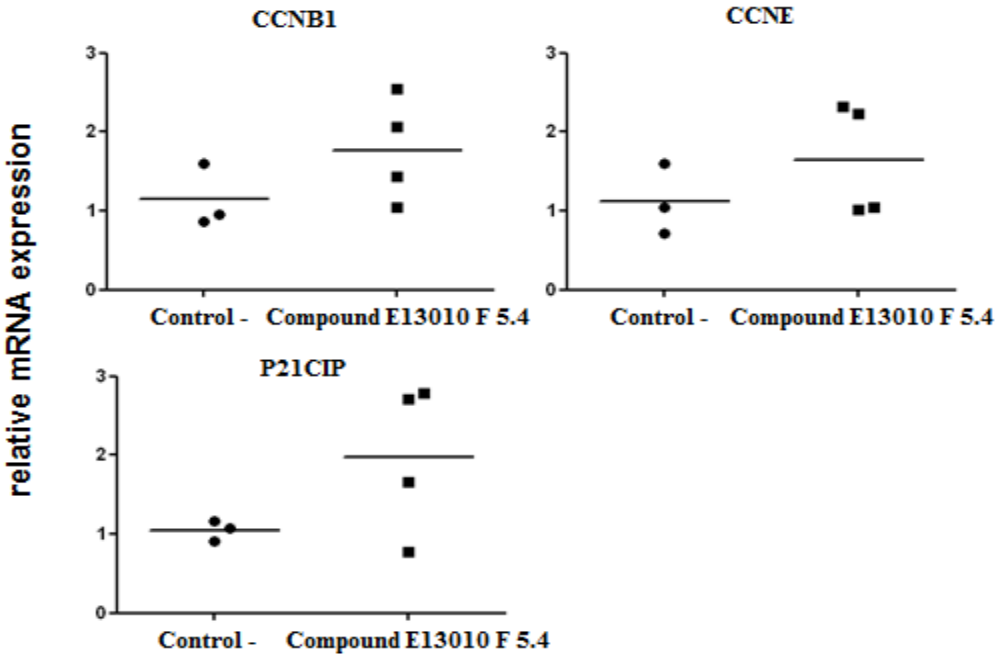

Figure 13 Relative mRNA expression from selected cell cycle genes CCNB1, CCNE, P21CIP treated with HT-29 cell lines.

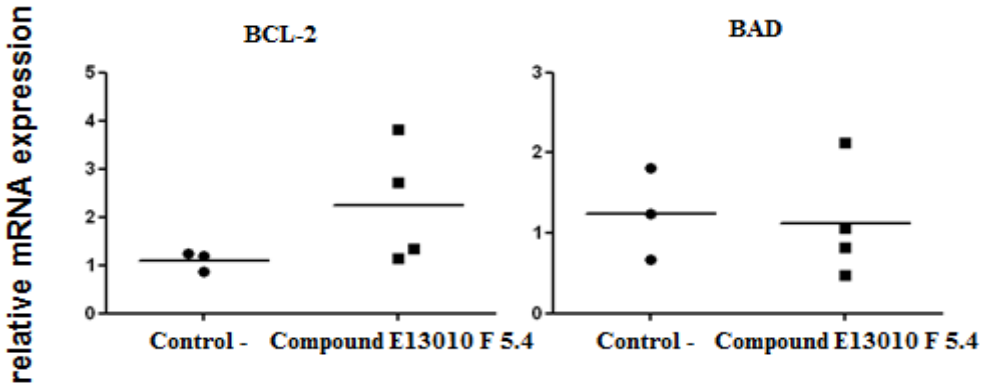

Figure 14 Relative mRNA expression from selected apoptosis genes, BCL-2 (anti-apoptotic) and BAD (pro-apoptotic) treated with HT-29 cell lines.

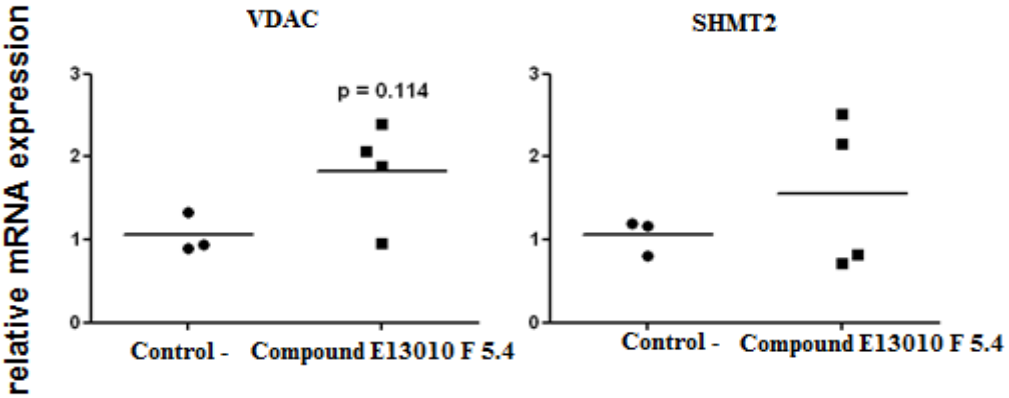

Figure 15 Relative mRNA expression from other cancer-related genes, VDAC and SHMT2 treated with HT-29 cell lines.

4. Proteomic Analysis

4.1. Protein extraction and quantification

The RKO and HT-29 cell lines were exposed to cyanobacteria compound, at a concentration of 30 µg/ mL and negative control with 1% DMSO. After 24 hours of exposure, proteins were extraction was performed as described in the materials and methods section. The Appendix 6, Table 19 indicates the concentration of protein extracted from each sample.

4.2. Two-dimensional Electrophoresis (2DGE)

Each protein extract was subjected to two-dimensional electrophoresis with a first phase isoelectric focusing followed by SDS-PAGE, the cells proteome to be resolved between isoelectric points 3 – 10. We performed a polyacrylamide gel (12.5%) for each protein extract (see protein concentration in Appendix 6, table 19) from each cell line and the respective control and treatment groups, in Figure 16 this is an example of a polyacrylamide gel.

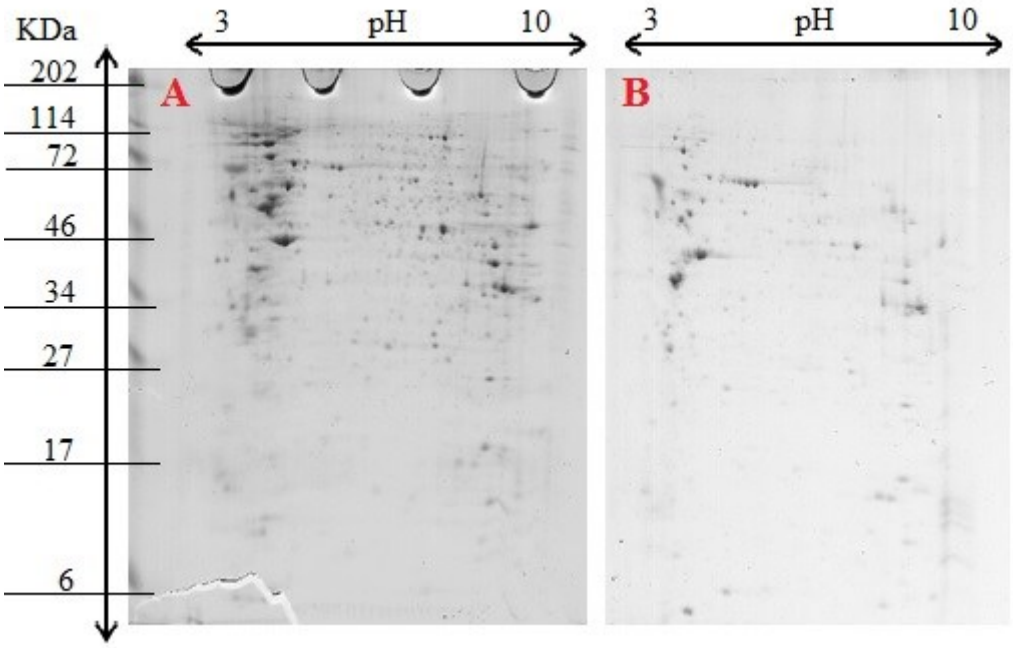

Figure 16 Polyacrylamide gel (12.5%) performed for the RKO (A) and HT-29 (B) cell line exposed at a concentration of 30 µg/mL of compound E13010 F 5.4.. The molecular weight of the gels between 202 and 6 KDa.

The polyacrylamide gels, a total of 16 (4 for each study group) were analysed by *PDQuest* (BioRad) software. Were identified 220 gel spots by the RKO cell line and 136 gel spots in the HT-29 cell line. The 95% confidence level for the *Student t-test* was used to identify differentially expressed spots between control and treatment groups yielding a total of 35 spots (see Appendix 7, Table 20) for cell line RKO and 26 spots (see Appendix 7, Table 21) for cell line HT-29.

In Figure 17, polyacrylamide gels (12.5%) are shown obtained for the cell line RKO treatment group exposed to 30 µg/mL of compound E13010 F 5.4 and negative control group with 1% DMSO.

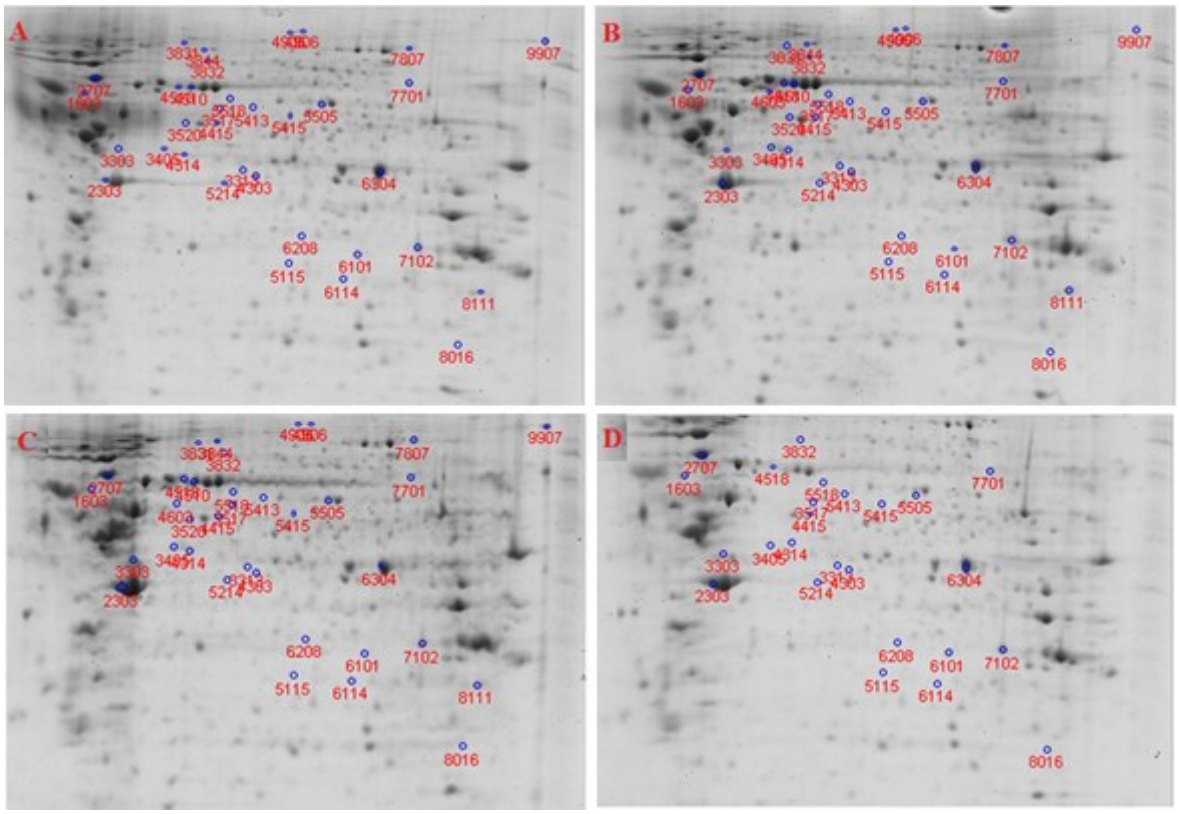

Figure 17 Polyacrylamide gels (12.5%) for the RKO cell line treatment group exposed to 30 µg/mL of compound E13010 F 5.4 and negative control (A – Replicate 1 treated with compound, B – Replicate 2 treated with compound, C – Replicate 3 treated with compound, D – Replicate 1 for negative control) indicating the relative position of spots identified by the *PDQuest* software, using the t-test with a confidence level of 95%.

In Figure 18, the polyacrylamide gels (12.5%) are shown obtained for the cell line HT-29 treatment group exposed to 30 µg/mL of compound E13010 F 5.4 and negative control group with 1% DMSO.

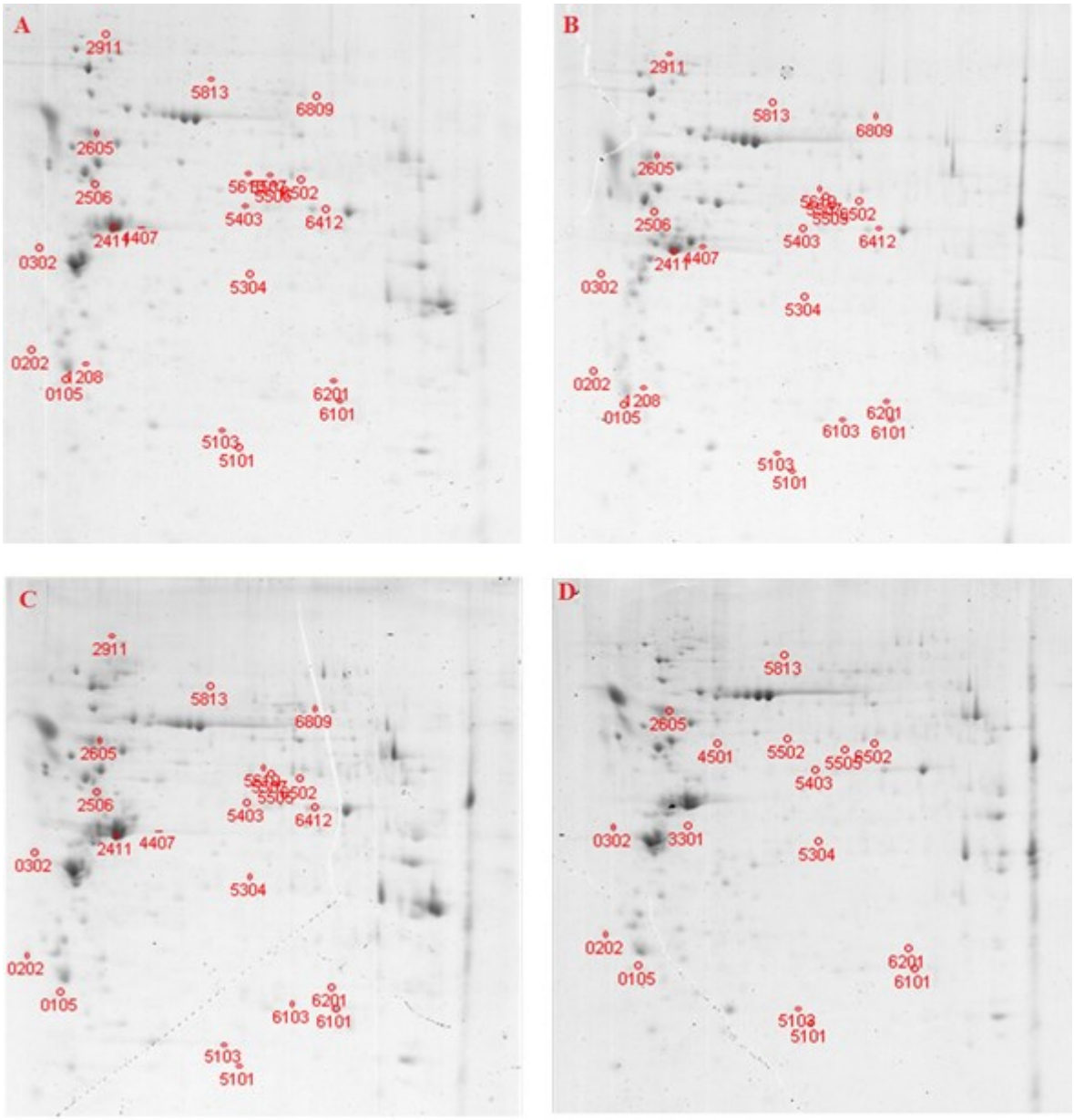

Figure 18 Polyacrylamide gels (12.5%) for the HT-29 cell line treatment group exposed to 30 µg/mL of compound E13010 F 5.4 and negative control (A – Replicate 1 treated with compound, B – Replicate 2 treated with compound, C – Replicate 3 treated with compound, D – Replicate 1 for negative control), indicating the relative position of spots identified by the *PDQuest* software, using the t-test with a confidence level of 95%.

4.3. Preparation of peptides for identification in matrix-assisted laser desorption ionization (MALDI) time-of-flight / time-of-flight (TOF/TOF)

From the 35 differentially expressed spots of cell line RKO identified by the *PDQuest* software, 16 spots were analysed so far by MALDI-TOF/TOF. Regarding the 26 spots of cell line HT-29, 5 spots were analysed so far by MALDI-TOF/TOF (Table 9).

Protein score is -10*Log(P), where P is the probability that the observed match is a random event. Protein scores greater than 65 are significant ($p<0.05$) and are derived from ions scores as a non-probabilistic basis for ranking protein hits.

Table 9 Spots analysed of RKO and HT-29 cell line.

Cell line	Spots	Cell line	Spots
RKO	2303	HT-29	202
	2707		2411
	3303		2605
	3313		4407
	3405		6101
	3517		
	3520		
	3831		
	3832		
	3844		
	4303		
	4510		
	5505		
	6304		
	7102		
	8111		

Only three spots were identified with statistical confidence, the spot 2707 and 6304 of RKO cell line and spot 2411 of HT-29 cell line. We conducted sequencing of the 25 peptide peaks having a relative noise signal sample and identified only two very similar proteins (Table 10).

Table 10 Identification of proteins by MALDI-TOF / TOF. For each protein is indicated name and accession number thereof by comparison with the UniProt database (84).

Spot	Accession	Protein name	Protein score	Function
2707	P11021	78 kDa glucose-regulated protein (*Homo sapiens*)	680	Facilitate the assembly multimeric proteins complex inside the endoplasmic reticulum.
	B4DEF7	cDNA FLJ60062, highly similar to 78 kDa glucose-regulated protein (*Homo sapiens*)	244	
6304	P06733	Alpha-enolase (*Homo sapiens*)	264	Stimulates immunoglobulin production and may be a tumour suppressor.
2411	B4DW52	cDNA FLJ55253, highly similar to Actin, cytoplasmic 1(*Homo sapiens*)	198	ATP binding.

Chapter V – Discussion

V.Discussion

The compound E13010 F 5.4 used in this work was previously isolated from the marine cyanobacteria strain *Synechocystis salina* LEGE 06099 (75). In order to get more biomass for new isolation of the compound the cyanobacteria strain was cultured in large scale. All the fractionating procedure, NMR analysis and TLC analysis were performed during this thesis.

Analysing all the results from the cytotoxicity assays, it was confirmed that cyanobacterial compound E13010 F 5.4 induced cytotoxicity that was more pronounced and dependent on the concentration on the cancer cell lines RKO and HT-29. Considering these results and due to the small amount of compound available only RKO and HT-29 cells lines were selected for the mRNA expression and proteomic analysis.

Overall, the analysis of mRNA expression indicated a significant variation compared to control for P21CIP, while a tendency of variation was present for BAD, BCL-2, CCNB1 and VDAC, however responses were different between both cell lines.

Analysis of mRNA expression genes of the RKO cells revealed a significant decrease of the P21CIP gene ($p < 0.05$). The P21CIP is a cell cycle regulator, which is involved in the anti-proliferation of cells by inhibiting cell cycle progression at the G1 to S phase (85, 86). The cyclin-dependent kinase inhibitor p21 promotes cell cycle arrest in response to many stimuli and, in many tumours, the increase of P21CIP resulted in a decreased ability of cells to divide. It also acts as a major effector of multiple tumour suppressor pathways to promoting anti-proliferative activity. The induction of P21CIP is a good indicator of growth arrest in colorectal cancer cells (85). Although the cyclin-dependent kinase inhibitor p21 was originally considered to be a tumor-suppressor it has been suggested that p21 may also act as an oncogene because it often inhibits apoptosis (80). Considering our results however the observed decrease of P21CIP mRNA expression is probably not related to the described effects above, but would indicate an increased proliferation, a decreased tumour suppression or reduction of the oncogene. At the moment, it is not clear how the observed effects connect to the induced cytotoxicity of the compound in the RKO cancer cell line.

Regarding the pro-apoptotic gene BAD, a non-significant decrease was observed in the RKO cell line ($p=0.087$) exposed to compound. In the literature it was demonstrated that

the relative levels of BCL-2 and BAD contribute to determine the drug resistance of colon tumour cells (87). The function of BAD is to regulate the phosphorylation state that modulates its protein–protein interactions and subcellular localization. Protein kinases phosphorylate BAD on serine residues. Phosphorylation at these sites enables BAD to bind with proteins and inhibits the binding of BAD with BCL-2, resulting in the inhibition of apoptosis. It is believed that apoptosis of cells is important in the pathogenesis of tumours (88). BCL-2 is an anti-apoptotic regulatory protein, but it also act as an inhibitor of proliferation. The function of BCL-2 in carcinogenesis is controversial, as the anti-apoptotic effect may be oncogenic while the anti-proliferative effect appears tumour-suppressive. This functions may be specific of tissue, so the prognostic implication of BCL-2 expression depends on cancer type (89). A decrease of the mRNA expression of pro-apoptotic gene BAD would indicate that maybe cells do not enter into apoptosis. This finding may also be supported by the increase in the expression of the gene CCNB1 since this gene encodes for cyclin B1, which is essential for the control of the cell cycle at the G2/M transition. The results may suggest a response of cells to fight against induced cytotoxicity. In RKO cell line, the gene CCNB1 is up-regulated, however, not statistically significant, which may indicate that cells proliferate and enter into the G2/M phase of the cell cycle. CCNB1 is a member of cyclin family involved in the quality control step of mitosis. It has been demonstrated that CCNB1 is involved in checkpoint control, whose dysfunction is an early event in carcinogenesis, and deregulated expression is observed in various human cancers like breast cancer, cervical cancer, lung cancer, esophageal squamous cell carcinoma, and melanoma (90). CCNB1 is overexpressed in the most human colorectal cancer tissues compared with the matched adjacent non tumours tissues. The literature suggested that CCNB1 promotes the proliferation of colorectal cancer cells *in vitro* and carcinogenesis *in vivo*, its mean CCNB1 exerts a growth-promoting function in human colorectal cancer. In short, it is believed that CCNB1 have an oncogenic role in colorectal cancer. CCNB1 is activated by checkpoint kinase 1 overexpression and inhibition of CCNB1 induces cell cycle arrest in different colorectal cancer cell lines through modulating the expression of G2/M cell cycle regulators. Suppression of CCNB1 induces apoptosis in a fewest colorectal cancer cells (90).

Regarding the analysis of mRNA expression of the genes of HT-29 cell line, we were faced with a difficulty that there were less replicates then in the RKO cell line (see chapter IV, section 3.2. Real-Time PCR). In this cell line, however, the genes CCNBI, P21CIP,

BCL-2 and VDAC (see chapter IV, section 4, Figure 13 – 15) showed a tendency to be increased although the values did not reach statistical significance.

As mentioned previously the gene CCNB1 is involved in mitosis checkpoint control, whose dysfunction is an early event in carcinogenesis, and deregulated expression is observed in various human cancers but the role of this gene is still unclear in colorectal cancer (90). The P21Cip is a cell cycle regulator, which is involved in the anti-proliferation of cells by inhibiting cell cycle progression at the G1 to S phase and is a good indicator of growth arrest in colorectal cancer cells (85, 86). BCL-2 is an anti-apoptotic regulatory protein, but it also an inhibitor of proliferation. Nevertheless, the function of BCL-2 in carcinogenesis is not clear (89). The voltage dependent anion channel (VDAC) is a class of porin ion channels located on the outer membrane of mitochondria. VDACs have an important role in mitochondria-mediated apoptosis. There is evidence that VDAC is involved in tumour progression. It was demonstrated that VDAC is up-regulated in tumour tissue in lung, breast, colon, liver, pancreatic, and thyroid cancers (91). In these case genes with functions in cell proliferation seem to be more expressed which may indicate an effort of cells to proliferate. It is assumed that a higher number of replicates would have resulted in significant alterations of these genes.

The analysis of the proteome by 2DGE resulted in differentially expressed spots for the RKO cell line and in differentially expressed spots for the HT-29 cell line. Apparently, the gel pictures of the proteomes of both cell lines were different, which indicated that major expressed proteins might be different considering their pH values and their molecular weight. The analysis of the altered proteins in response to the exposure to the compound already indicated that different responses were present in both selected cancer cell lines. Differentially expressed spots had a different profile regarding their molecular weight and pH, as separated in the 2DGE. In order to identify those spots, we forwarded them to peptide identification by MALDI-TOF/TOF. Of the 21 spots analysed, only four proteins could be identified with statistical significance, spot 2707, the 78 kDa glucose-regulated protein (GRP78), cDNA FLJ60062, highly similar to 78 kDa glucose-regulated protein (in RKO); spot 6304, Alpha-enolase (EnoA; in RKO); spot 2411, cDNA FLJ55253, highly similar to Actin, cytoplasmic 1 (in HT29). Both GRP78 and EnoA were decreased in RKO cell line, while actin was increased in HT-29 (Appendix 7).

Typically, human colon cancer cells have hypoglycemic and hypoxic centres due to incomplete vasculature, which results in an increased glucose uptake, and glycolysis as an important energy source (92). GRP78 is significantly increased in colon tumours compared to normal mucosa, suggesting that up-regulation of GRP78 can be a marker of malignant transformation, but is not a useful prognostic marker (87). 78 kDa glucose-regulated protein is a member of the 70 kDa heat shock family of stress proteins, resident in the endoplasmic reticulum, and participate in assembly and integral membrane proteins (87). This protein has been implicated in the development of tumorigenicity, drug resistance, and cytotoxic immunology. The cellular changes in solid tumours *in vivo*, such as hypoxia, glucose deprivation and alterations in calcium flux may result in an accumulation of unfolded proteins and/or deformation of the lumen of the endoplasmic reticulum (ER), and may impair the function of the ER-Golgi network (88, 89). Angiogenesis regulates the degradation of extracellular basement membrane of the original vessel proliferation and formation of new capillaries (90). The glucose-regulated proteins (GRP) are a group of proteins, whose synthesis was increased in the cells deprived of glucose (87). GRP78 is a major pro-angiogenic chaperone protein, mainly found in the ER lumen, and promotes tumour proliferation, survival, angiogenesis and resistance of chemotherapy (90). GRP78 protects tumour cells against the toxic effects of anticancer agents *in vitro*, and concordantly the induction of GRP78 can protect tumour cells *in vivo*. GRP78 levels are high in various cancer cell lines, solid tumours and human cancers biopsies, and appear to correlate with malignancy. Furthermore, GRP78 induction protects cancer cells from immune surveillance, while suppression of GRP78 improved apoptosis-inhibited tumour growth and increased the cytotoxicity of chronically hypoxic cells.

In the line of the above described knowledge, a decreased presence of the GRP78 protein as observed in this study in the RKO cell line could be involved in the mechanism leading to a shortage in glucose supply, and reduced proliferation and survival of colon cancer cells (93).

Another protein identified by MALDI-TOF/TOF was alpha-enolase. Enolase (ENOA; 2-phospho-D-glycerate hydrolase) is a very ubiquitous conserved cytosolic metalloenzyme with a molecular weight of 48 kDa. It catalyzes the dehydration of 2-phospho-D-glycerate to phosphoenolpyruvate in the glycolytic pathway. It exists in three different isoforms, alpha, beta, and gamma based on three independent loci (91). Alpha-enolase was present in almost all adult tissues, beta-enolase was expressed in muscle tissues, and gamma-enolase

was found in neurons and neuroendocrine cells. EnoA was known as a very important glycolytic enzyme, responsible for catalysing the dehydration of 2-phosphoglycerate to phosphoenolpyruvate in the final steps of glycolysis and been implicated in many other biological and physiological processes (92). EnoA has been detected on the surface of vascular endothelium, various cell types including monocytes, macrophages, B cells and T cells and is recognized as a plasminogen receptor. EnoA as a tumour associated antigen pancreatic ductal adenocarcinoma and a moonlighting protein that works both as a glycolytic enzyme and as a membrane plasminogen receptor, thus promoting tumour proliferation (93). Furthermore, EnoA is believed to have the function of a tumour suppressor. In tumour cells, is up regulated and supports anaerobic proliferation (94). In our study, EnoA is significantly decreased and could be involved in a decreased rate of glycolysis, where it catalyses the final step. Interestingly, both altered and identified proteins in the RKO cell line exposed to compound E13010 F 5.4 indicate alterations in the glycolysis, which may lead to a shortage in energy supply.

The third identified protein was cDNA FLJ55253, highly similar to Actin, cytoplasmic 1 or Beta-actin. In all eukaryotic cells, actin family involves highly conservative proteins. Actin has different functions in the cell, including cell motility, contractile ring formation during cytokinesis, conservation of cell shape, signal transduction, cell adhesion, transcription and muscle contraction. In vertebrates, six actin isoforms are expressed. They were classified according to the isoelectric point and primary tissue or cellular location and comprise β- and γ-cytoplasmic, α-skeletal, α-cardiac, and α- and γ-smooth muscle isoactins. Mammalian erythrocytes comprehend only β-actin. Actin isoforms are products of separate genes, but there is a similarity in their nucleotide sequences that result in the primary structure of the protein. The differences between the actin isoform are more variable in the N-terminal region of actin molecule. Changes in the levels of actin isoforms in cells are often associated with pathological processes. It has been demonstrated that abnormal levels of β- and γ-actins was present in many tumour types like chemically induced melanoma, hepatoma, lymphoma, and breast cancer. Cytoplasmic β-actin appears to be over-expressed in many tumours, especially actively moving cancers cells. This isoform level was also significantly increased in some cases, highly invasive variants of colon cancer cells, MDCK cells transformed by Moloney sarcoma virus or melanoma cells T1C1 (95). Primary canonical pathway analyses identified actin-cytoskeleton pathway to be of great relevance, and expressively disrupted in the progression of normal colonic mucosa. The

actin-cytoskeleton pathway is a very important component in the movement of cells, and it is supposed to represent the backbone of cells that allow cell migration and mobility within the body. The actin-cytoskeleton pathway has already connected in the development and pathogenesis of invasive metastatic sporadic CRC. New studies have suggested that actin-cytoskeleton pathway can be involved in the metastasis sporadic CRC through cytoskeletal proteins such as Fascin-1. The importance of disturbance of the actin-cytoskeleton pathway in the CRC is very interesting, especially since the detection of this deregulated pathway can provide a new screening and therapeutic target (96).

Problems were met in the identification of peptide peaks due to the appearance of strong contamination peaks during the analysis. A re-identification of the spots is thereby necessary, after elimination of the unknown source of contamination. Since bacterial and fungal contamination could be excluded by the proteome analysis, currently plastic polymers are the main suspected contamination source. Therefore, the main interpretation of proteomic results has to be delayed until positive identification of differentially expressed spots by MALDI-TOF/TOF.

Chapter VI – Conclusion

VI. Conclusion

In this work we aim to infer about the potential of a marine cyanobacteria compound as an anticancer agent. By analysing the expression of genes involved in cell cycle and apoptosis and by applying a proteomic approach we aimed to reveal molecular and biochemical mechanisms involved in its cytotoxicity in cancer cell lines. In this analysis, the target gene with significant alteration was P21CIP, while a tendency of alteration was observed for BAD, BCL-2, CCNB1 and VDAC, though differences between the two cell lines were evident. The alteration of mRNA expression level of P21CIP, BAD and CCNB1 in RKO cells may indicate an increased proliferation, a decrease of pro-apoptotic protein level and entrance into the G2/M phase. However, reduced P21CIP level could be also indicative of reduced oncogene level. In HT-29 cell, no significant alterations were observed, but a similar tendency was present for induced cell proliferation (BCL-2, CCNB1). Nevertheless, increased VDAC mRNA expression may indicate higher permeability of mitochondria. Although results seem preliminary and need confirmation, it is clear that mechanisms are involved in cell death and proliferation, which may appear as counter-regulation to the exposure.

By peptide identification, three proteins have been identified: 78 kDa glucose-regulated protein; cDNA FLJ60062, highly similar to 78 kDa glucose-regulated protein; Alpha-enolase; cDNA FLJ55253, highly similar to Actin, cytoplasmic 1. The apparent decrease of GRP78 and EnoA in RKO cells may indicate a reduction in glycolysis and thereby a shortage of important energy supply. In addition, the protein 78 kDa glucose-regulated has been implicated in the development of tumorigenicity, drug resistance, and cytotoxic immunology. Alpha-enolase is believed to have the function of tumour suppressor. The protein cDNA FLJ55253, highly similar to Actin, cytoplasmic 1 was increased in HT29 cells, and alterations of the cytoskeleton is a known anti-cancer target.

The repetition of assays during this project was limited by the small amount of the pure compound that was available. Further purification of the compound is ongoing, which will enable future studies that will deliver novel insights into the molecular mechanism of action of compound.

Chapter VII – References

VII. References

1. Costa MS, Costa M, Ramos V, Leão PN, Barreiro A, Vasconcelos V, et al. Picocyanobacteria From a Clade of Marine Cyanobium Revealed Bioactive Potential Against Microalgae, Bacteria, and Marine Invertebrates. Journal of Toxicology and Environmental Health, Part A. 2015;78(7):432-42.
2. Brito Â, Gaifem J, Ramos V, Glukhov E, Dorrestein PC, Gerwick WH, et al. Bioprospecting Portuguese Atlantic coast cyanobacteria for bioactive secondary metabolites reveals untapped chemodiversity. Algal Research. 2015;9(0):218-26.
3. Costa M, Garcia M, Costa-Rodrigues J, Costa MS, Ribeiro MJ, Fernandes MH, et al. Exploring Bioactive Properties of Marine Cyanobacteria Isolated from the Portuguese Coast: High Potential as a Source of Anticancer Compounds. Marine drugs. 2013;12(1):98-114.
4. Martins J, Leão PN, Ramos V, Vasconcelos V. N-terminal protease gene phylogeny reveals the potential for novel cyanobactin diversity in cyanobacteria. Marine drugs. 2013;11(12):4902-16.
5. Hagemann M. Molecular biology of cyanobacterial salt acclimation. FEMS microbiology reviews. 2011;35(1):87-123.
6. Mereschkowsky C. Über natur und ursprung der chromatophoren im pflanzenreiche1905.
7. Margulis L. Origin of eukaryotic cells: evidence and research implications for a theory of the origin and evolution of microbial, plant, and animal cells on the Precambrian earth: Yale University Press New Haven; 1970.
8. Deusch O, Landan G, Roettger M, Gruenheit N, Kowallik KV, Allen JF, et al. Genes of cyanobacterial origin in plant nuclear genomes point to a heterocyst-forming plastid ancestor. Molecular biology and evolution. 2008;25(4):748-61.
9. Tandeau de Marsac N, Houmard J. Adaptation of cyanobacteria to environmental stimuli: new steps towards molecular mechanisms. FEMS Microbiology Letters. 1993;104(1-2):119-89.
10. Brito Â, Ramos V, Seabra R, Santos A, Santos CL, Lopo M, et al. Culture-dependent characterization of cyanobacterial diversity in the intertidal zones of the Portuguese coast: A polyphasic study. Systematic and Applied Microbiology. 2012;35(2):110-9.
11. Whitton BA. Cyanobacterial diversity in relation to the environment. Algal Toxins: Nature, Occurrence, Effect and Detection: Springer; 2008. p. 17-43.
12. Lopes VR, Ramos V, Martins A, Sousa M, Welker M, Antunes A, et al. Phylogenetic, chemical and morphological diversity of cyanobacteria from Portuguese temperate estuaries. Marine environmental research. 2012;73:7-16.
13. Knoll AH. Cyanobacteria and earth history. The Cyanobacteria: Molecular Biology, Genomics, and Evolution. 2008:1-20.
14. Sode K, Tatara M, Takeyama H, Burgess JG, Matsunaga T. Conjugative gene transfer in marine cyanobacteria: Synechococcus sp., Synechocystis sp. and Pseudanabaena sp. Applied microbiology and biotechnology. 1992;37(3):369-73.
15. Antonopoulou S, Karantonis HC, Nomikos T, Oikonomou A, Fragopoulou E, Pantazidou A. Bioactive polar lipids from *Chroococcidiopsis* sp. (Cyanobacteria). Comparative Biochemistry and Physiology Part B: Biochemistry and Molecular Biology. 2005;142(3):269-82.

16. Ehrenreich IM, Waterbury JB, Webb EA. Distribution and diversity of natural product genes in marine and freshwater cyanobacterial cultures and genomes. Applied and environmental microbiology. 2005;71(11):7401-13.
17. Harada K-i. Production of secondary metabolites by freshwater cyanobacteria. Chemical and Pharmaceutical bulletin. 2004;52(8):889-99.
18. Costa M, Costa-Rodrigues J, Fernandes MH, Barros P, Vasconcelos V, Martins R. Marine cyanobacteria compounds with anticancer properties: A review on the implication of apoptosis. Marine drugs. 2012;10(10):2181-207.
19. Mayer AMS, Glaser KB, Cuevas C, Jacobs RS, Kem W, Little RD, et al. The odyssey of marine pharmaceuticals: a current pipeline perspective. Trends in pharmacological sciences. 2010;31(6):255-65.
20. Alquezar R, Anastasi A. The Use of the Cyanobacteria, Cyanobium sp., as a Suitable Organism for Toxicity Testing by Flow Cytometry. Bulletin of environmental contamination and toxicology. 2013;90(6):684-90.
21. Watanabe MM, Nakagawa M, Katagiri M, Aizawa Ki, Hiroki M, Nozaki H. Purification of freshwater picoplanktonic cyanobacteria by pour-plating in 'ultra-low-gelling-temperature agarose'. Phycological Research. 1998;46(s2):71-5.
22. Jezberová J, Komárková J. Morphometry and growth of three Synechococcus-like picoplanktic cyanobacteria at different culture conditions. Hydrobiologia. 2007;578(1):17-27.
23. Sieburth J, Smetacek V, Lenz J. Pelagic ecosystem structure: heterotrophic compartments of the plankton and their relationship to plankton size fractions. Limnol Oceanogr. 1978;23(6):1256-63.
24. Callieri C, Stockner JG. Freshwater autotrophic picoplankton: a review. Journal of Limnology. 2002;61(1):1-14.
25. Bird D, Kalff J. Empirical relationships between bacterial abundance and chlorophyll concentration in fresh and marine waters. Canadian Journal of Fisheries and Aquatic Sciences. 1984;41(7):1015-23.
26. Bell T, Kalff J. The contribution of picophytoplankton in marine and freshwater systems of different trophic status and depth. Limnology and Oceanography. 2001;46(5):1243-8.
27. Stockner JG. Phototrophic picoplankton: An overview from marine and freshwater ecosystems. Limnology and Oceanography. 1988;33(4):765-75.
28. Cole JJ, Findlay S, Pace ML. Bacterial production in fresh and saltwater ecosystems: a cross-system overview. Marine ecology progress series Oldendorf. 1988;43(1):1-10.
29. Drakare S. Competition between picoplanktonic cyanobacteria and heterotrophic bacteria along crossed gradients of glucose and phosphate. Microbial ecology. 2002;44(4):327-35.
30. Rippka R, Cohen-Bazire G, editors. The cyanobacteriales: A legitimate order based on the type strain *Cyanobacterium stanieri?* Annales de l'Institut Pasteur/Microbiologie; 1983: Elsevier.
31. Hamilton TJ, Paz-Yepes J, Morrison RA, Palenik B, Tresguerres M. Exposure to bloom-like concentrations of two marine Synechococcus cyanobacteria (strains CC9311 and CC9902) differentially alters fish behaviour. *Conservation Physiology*. 2014;*2*(1):1-9.
32. Li WK, Wood AM. Vertical distribution of North Atlantic ultraphytoplankton: analysis by flow cytometry and epifluorescence microscopy. Deep Sea Research Part A Oceanographic Research Papers. 1988;35(9):1615-38.

33. Olson RJ, Chisholm SW, Zettler ER, Altabet MA, Dusenberry JA. Spatial and temporal distributions of prochlorophyte picoplankton in the North Atlantic Ocean. Deep Sea Research Part A Oceanographic Research Papers. 1990;37(6):1033-51.
34. Campbell L, Nolla H, Vaulot D. The importance of Prochlorococcus to community structure in the central North Pacific Ocean. Oceanographic Literature Review. 1995;42(5).
35. Urbach E, Scanlan DJ, Distel DL, Waterbury JB, Chisholm SW. Rapid diversification of marine picophytoplankton with dissimilar light-harvesting structures inferred from sequences of Prochlorococcus and Synechococcus (Cyanobacteria). Journal of molecular evolution. 1998;46(2):188-201.
36. Stanier R, Kunisawa R, Mandel M, Cohen-Bazire G. Purification and properties of unicellular blue-green algae (order Chroococcales). Bacteriological reviews. 1971;35(2):171.
37. Watanabe M, Suda S, Kasai F, Sawaguchi T. Axenic cultures of the three species of Microcystis (Cyanophyta= Cyanobacteria). Bull JFCC. 1985;1:57-63.
38. Rippka R. Isolation and purification of cyanobacteria. Methods in enzymology. 1988;167:3.
39. Castenholz RW. [3] Culturing methods for cyanobacteria. Methods in enzymology. 1988;167:68-93.
40. Bolch CJ, Blackburn SI. Isolation and purification of Australian isolates of the toxic cyanobacteriumMicrocystis aeruginosa Kütz. Journal of Applied Phycology. 1996;8(1):5-13.
41. Jensen PR, Fenical W. Marine bacterial diversity as a resource for novel microbial products. Journal of Industrial Microbiology. 1996;17(5-6):346-51.
42. Cragg GM, Newman DJ, Snader KM. Natural Products in Drug Discovery and Development. Journal of Natural Products. 1997;60(1):52-60.
43. Sone H, Kondo T, Kiryu M, Ishiwata H, Ojika M, Yamada K. Dolabellin, a Cytotoxic Bisthiazole Metabolite from the Sea Hare *Dolabella auricularia*: Structural Determination and Synthesis. Journal of Organic Chemistry. 1995;60(15):4774-81.
44. Nakao Y, Yoshida WY, Szabo CM, Baker BJ, Scheuer PJ. More Peptides and Other Diverse Constituents of the Marine Mollusk *Philinopsis speciosa*. Journal of Organic Chemistry. 1998;63(10):3272-80.
45. Davidson BS. New dimensions in natural products research: cultured marine microorganisms. Current Opinion in Biotecnology. 1995;6(3):284-91.
46. Patterson GML, Baldwin CL, Bolis CM, Caplan FR, Karuso H, Larsen LK, et al. Antineoplastic activity of cultured blue-green algae (cyanophyta). Journal of Phycology. 1991;27(4):530-6.
47. Patterson GML, Baker KK, Baldwin CL, Bolis CM, Caplan FR, Larsen LK, et al. Antiviral activity of cultured blue-green algae (cyanophyta). Journal of Phycology. 1993;29(1):125-30.
48. Jaiswal P, Singh PK, Prasanna R. Cyanobacterial bioactive molecules--an overview of their toxic properties.(Report). Canadian Journal of Microbiology. 2008;54(9):701.
49. Mundt S, Kreitlow S, Nowotny A, Effmert U. Biochemical and pharmacological investigations of selected cyanobacteria. Int J Hyg Environ Health. 2001;203(4):327-34.
50. Berry JP, Gantar M, Perez MH, Berry G, Noriega FG. Cyanobacterial Toxins as Allelochemicals with Potential Applications as Algaecides, Herbicides and Insecticides. Marine Drugs. 2008;6(2):117-46.

51. Lopes VR, Vasconcelos VM. Bioactivity of benthic and picoplanktonic estuarine cyanobacteria on growth of photoautotrophs: inhibition versus stimulation. Marine drugs. 2011;9(5):790-802.
52. Martins RF, Ramos MF, Herfindal L, Sousa JA, Skærven K, Vasconcelos VM. Antimicrobial and Cytotoxic Assessment of Marine Cyanobacteria - Synechocystis and Synechococcus. Marine Drugs. 2008;6(1):1-11.
53. Burja AM, Banaigs B, Abou-Mansour E, Grant Burgess J, Wright PC. Marine cyanobacteria—a prolific source of natural products. Tetrahedron. 2001;57(46):9347-77.
54. Skulberg OM, Skulberg R, Carmichael WW, Andersen RA, Matsunaga S, Moore RE. Investigations of a neurotoxic oscillatorialean strain (Cyanophyceae) and its toxin. Isolation and characterization of homoanatoxin- a. Environmental Toxicology and Chemistry. 1992;11(3):321-9.
55. Scott WE. Occurrence and significance of toxic cyanobacteria in Southern Africa. Water Science & Technology. 1991;23(1-3):175-80.
56. Gerwick WH, Moore BS. Lessons from the past and charting the future of marine natural products drug discovery and chemical biology. Chemistry & biology. 2012;19(1):85-98.
57. Tan LT. Bioactive natural products from marine cyanobacteria for drug discovery. Phytochemistry. 2007;68(7):954-79.
58. Taniguchi M, Nunnery JK, Engene N, Esquenazi E, Byrum T, Dorrestein PC, et al. Palmyramide A, a Cyclic Depsipeptide from a Palmyra Atoll Collection of the Marine Cyanobacterium Lyngbya majuscula. J Nat Prod. 2010;73(3):393-8.
59. McPhail KL, Correa J, Linington RG, González J, Ortega-Barría E, Capson TL, et al. Antimalarial linear lipopeptides from a Panamanian strain of the marine cyanobacterium Lyngbya majuscula. Journal of natural products. 2007;70(6):984-8.
60. Matthew S, Paul VJ, Luesch H. Largamides A–C, tiglic acid-containing cyclodepsipeptides with elastase-inhibitory activity from the marine cyanobacterium Lyngbya confervoides. Planta medica. 2009;75(5):528.
61. Lopes VR, Fernández N, Martins RF, Vasconcelos V. Primary screening of the bioactivity of brackishwater cyanobacteria: Toxicity of crude extracts to Artemia salina larvae and Paracentrotus lividus embryos. Marine drugs. 2010;8(3):471-82.
62. Leão PN, Costa M, Ramos V, Pereira AR, Fernandes VC, Domingues VF, et al. Antitumor activity of hierridin B, a cyanobacterial secondary metabolite found in both filamentous and unicellular marine strains. PloS one. 2013;8(7):e69562.
63. Martins R, Pereira P, Welker M, Fastner J, Vasconcelos VM. Toxicity of culturable cyanobacteria strains isolated from the Portuguese coast. Toxicon. 2005;46(4):454-64.
64. Frazão B, Martins R, Vasconcelos V. Are known cyanotoxins involved in the toxicity of picoplanktonic and filamentous North Atlantic marine cyanobacteria? Marine drugs. 2010;8(6):1908-19.
65. Martins R, Fernandez N, Beiras R, Vasconcelos V. Toxicity assessment of crude and partially purified extracts of marine *Synechocystis* and *Synechococcus* cyanobacterial strains in marine invertebrates. Toxicon. 2007;50(6):791-9.
66. Lopes VR, Schmidtke M, Helena Fernandes M, Martins R, Vasconcelos V. Cytotoxicity in L929 fibroblasts and inhibition of herpes simplex virus type 1 Kupka by estuarine cyanobacteria extracts. Toxicology in Vitro. 2011;25(4):944-50.

67. Li B, Sher D, Kelly L, Shi Y, Huang K, Knerr PJ, et al. Catalytic promiscuity in the biosynthesis of cyclic peptide secondary metabolites in planktonic marine cyanobacteria. Proceedings of the National Academy of Sciences. 2010;107(23):10430-5.
68. Donia MS, Fricke WF, Partensky F, Cox J, Elshahawi SI, White JR, et al. Complex microbiome underlying secondary and primary metabolism in the tunicate-Prochloron symbiosis. Proceedings of the National Academy of Sciences. 2011;108(51):E1423-E32.
69. Shih PM, Wu D, Latifi A, Axen SD, Fewer DP, Talla E, et al. Improving the coverage of the cyanobacterial phylum using diversity-driven genome sequencing. Proceedings of the National Academy of Sciences. 2013;110(3):1053-8.
70. Jemal A, Bray F, Center MM, Ferlay J, Ward E, Forman D. Global cancer statistics. CA: a cancer journal for clinicians. 2011;61(2):69-90.
71. Roychoudhuri R, Robinson D, Putcha V, Cuzick J, Darby S, Møller H. Increased cardiovascular mortality more than fifteen years after radiotherapy for breast cancer: a population-based study. BMC cancer. 2007;7(1):9.
72. Li X, Roginsky AB, Ding XZ, Woodward C, Collin P, Newman RA, et al. Review of the Apoptosis Pathways in Pancreatic Cancer and the Anti-apoptotic Effects of the Novel Sea Cucumber Compound, Frondoside A. Annals of the New York Academy of Sciences. 2008;1138(1):181-98.
73. Kang U-B, Yeom J, Kim H-J, Kim H, Lee C. Expression profiling of more than 3500 proteins of MSS-type colorectal cancer by stable isotope labeling and mass spectrometry. Journal of proteomics. 2012;75(10):3050-62.
74. Warburg O. On the origin of cancer cells. Science. 1956;123(3191):309-14.
75. Wong N, De Melo J, Tang D. PKM2, a central point of regulation in cancer metabolism. International journal of cell biology. 2013;2013.
76. Chandra D, Singh KK. Genetic insights into OXPHOS defect and its role in cancer. Biochimica et Biophysica Acta (BBA)-Bioenergetics. 2011;1807(6):620-5.
77. Liou S-F, Lin H-H, Liang J-C, Chen J, Yeh J-L. Inhibition of human prostate cancer cells proliferation by a selective alpha1-adrenoceptor antagonist labedipinedilol-A involves cell cycle arrest and apoptosis. Toxicology. 2009;256(1):13-24.
78. Hanahan D, Weinberg RA. Hallmarks of cancer: the next generation. cell. 2011;144(5):646-74.
79. van der Zee JA, van Eijck CHJ, Hop WCJ, van Dekken H, Dicheva BM, Seynhaeve ALB, et al. Angiogenesis: A prognostic determinant in pancreatic cancer? European Journal of Cancer. 2011;47(17):2576-84.
80. Afonso T. Bioassay-guided isolation of cyanobacterial metabolites with anticancer activity: Instituto de Ciências Biomédicas Abel Salazar, Universidade do Porto; 2014.
81. Freitas S. Toxicological Assessment of Marine Cyanobacterial Extracts in Human Tumor Cell Lines - Proteomic and Gene Expression Approach: Institute of Biomedical Sciences of Abel Salazar from the University of Porto.; 2013.
82. National Center for Biotechnology Information Nacional Library of Medicine [Available from: http://www.ncbi.nlm.nih.gov/.
83. Berridge MV, Tan AS. Characterization of the Cellular Reduction of 3-(4,5-dimethylthiazol-2-yl)-2,5-diphenyltetrazolium bromide (MTT): Subcellular Localization, Substrate Dependence, and Involvement of Mitochondrial Electron Transport in MTT Reduction. Archives of Biochemistry and Biophysics. 1993;303(2):474-82.
84. Consortium U. UniProt 2015 [Available from: http://www.uniprot.org/.

85. Kim J-A, Park K-S, Kim H-I, Oh S-Y, Ahn Y, Oh J-W, et al. Troglitazone activates p21 Cip/WAF1 through the ERK pathway in HCT15 human colorectal cancer cells. Cancer letters. 2002;179(2):185-95.
86. Lee J-H, Lee J-S, Kim S-E, Moon B-S, Kim Y-C, Lee S-K, et al. Tautomycetin inhibits growth of colorectal cancer cells through p21cip/WAF1 induction via the extracellular signal–regulated kinase pathway. Molecular cancer therapeutics. 2006;5(12):3222-31.
87. Hassankhani R, Sam MR, Esmaeilou M, Ahangar P. Prodigiosin isolated from cell wall of Serratia marcescens alters expression of apoptosis-related genes and increases apoptosis in colorectal cancer cells. Medical Oncology. 2015;32(1):1-8.
88. Kim MR, Jeong EG, Chae B, Lee JW, Soung YH, Nam SW, et al. Pro-apoptotic PUMA and anti-apoptotic phospho-BAD are highly expressed in colorectal carcinomas. Digestive diseases and sciences. 2007;52(10):2751-6.
89. Fernandes ATG, Rocha NP, Vendrame E, Russomano F, Grinsztejn BJ, Friedman RK, et al. Polymorphism in apoptotic BAX (-248G> A) gene but not in anti-apoptotic BCL2 (-938C> A) gene and its protein and mRNA expression are associated with cervical intraepithelial neoplasia. Apoptosis. 2015;20(10):1347-57.
90. Fang Y, Yu H, Liang X, Xu J, Cai X. Chk1-induced CCNB1 overexpression promotes cell proliferation and tumor growth in human colorectal cancer. Cancer biology & therapy. 2014;15(9):1268-79.
91. Ko J-H, Gu W, Lim I, Zhou T, Bang H. Expression profiling of mitochondrial voltage-dependent anion channel-1 associated genes predicts recurrence-free survival in human carcinomas. 2014.
92. Park H-R, Ryoo I-J, Choo S-J, Hwang J-H, Kim J-Y, Cha M-R, et al. Glucose-deprived HT-29 human colon carcinoma cells are sensitive to verrucosidin as a GRP78 down-regulator. Toxicology. 2007;229(3):253-61.
93. Mhaidat N, Alzoubi K, Khabour O, Banihani M, Al-Balas Q, Swaidan S. GRP78 regulates sensitivity of human colorectal cancer cells to DNA targeting agents. Cytotechnology. 2014:1-9.

Chapter VIII – Appendix

VIII. Appendix

Appendix 1 – Nuclear Magnetic Resonance spectroscopy

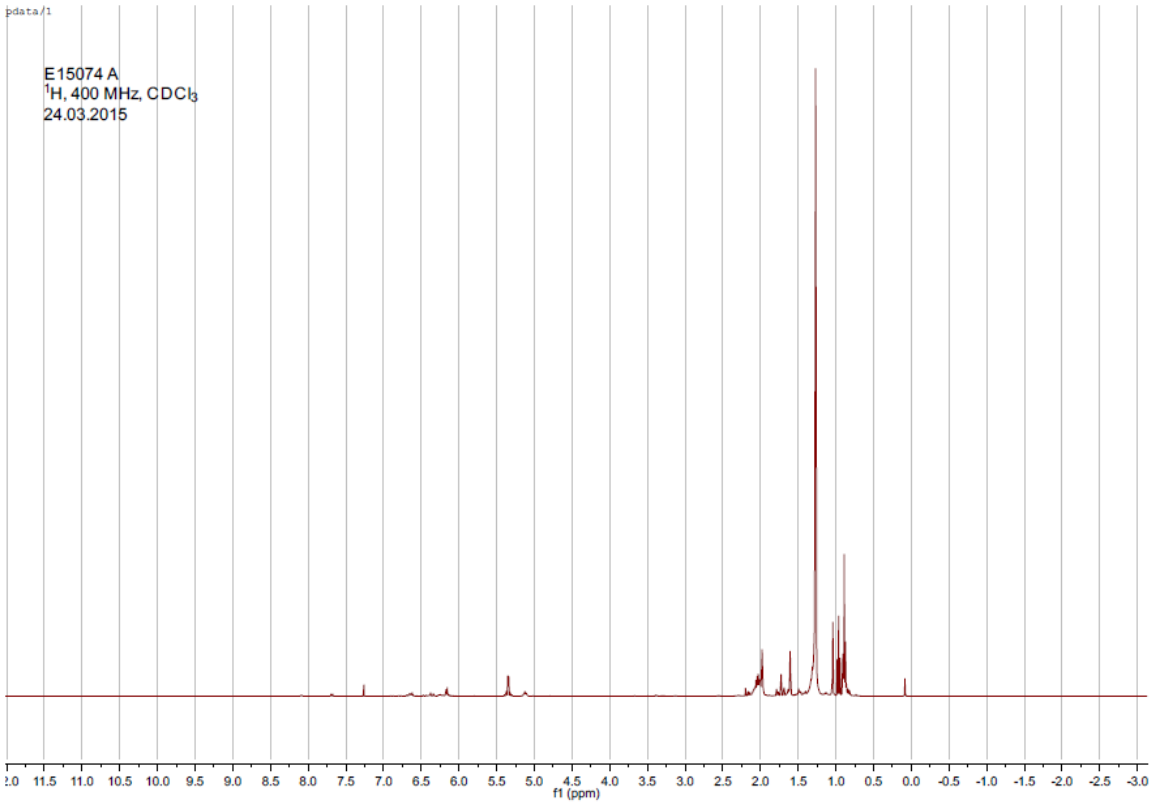

Figure 19 Fraction A.

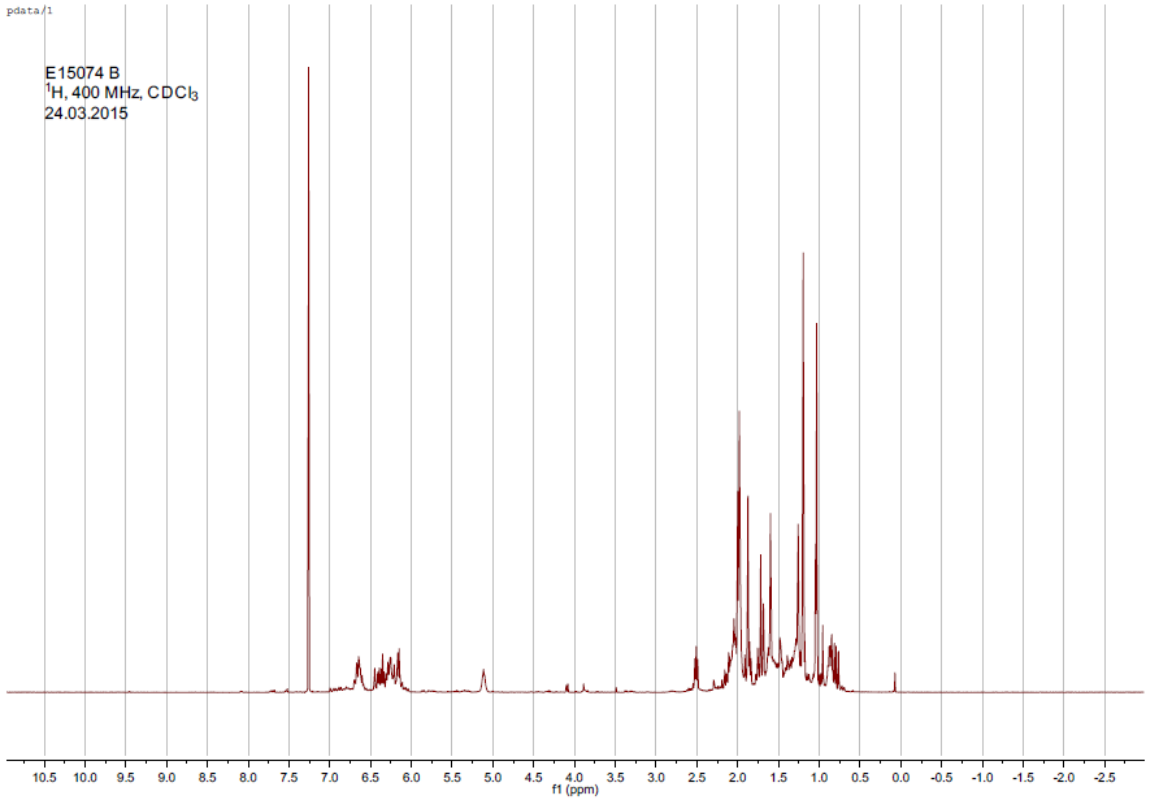

Figure 20 Fraction B.

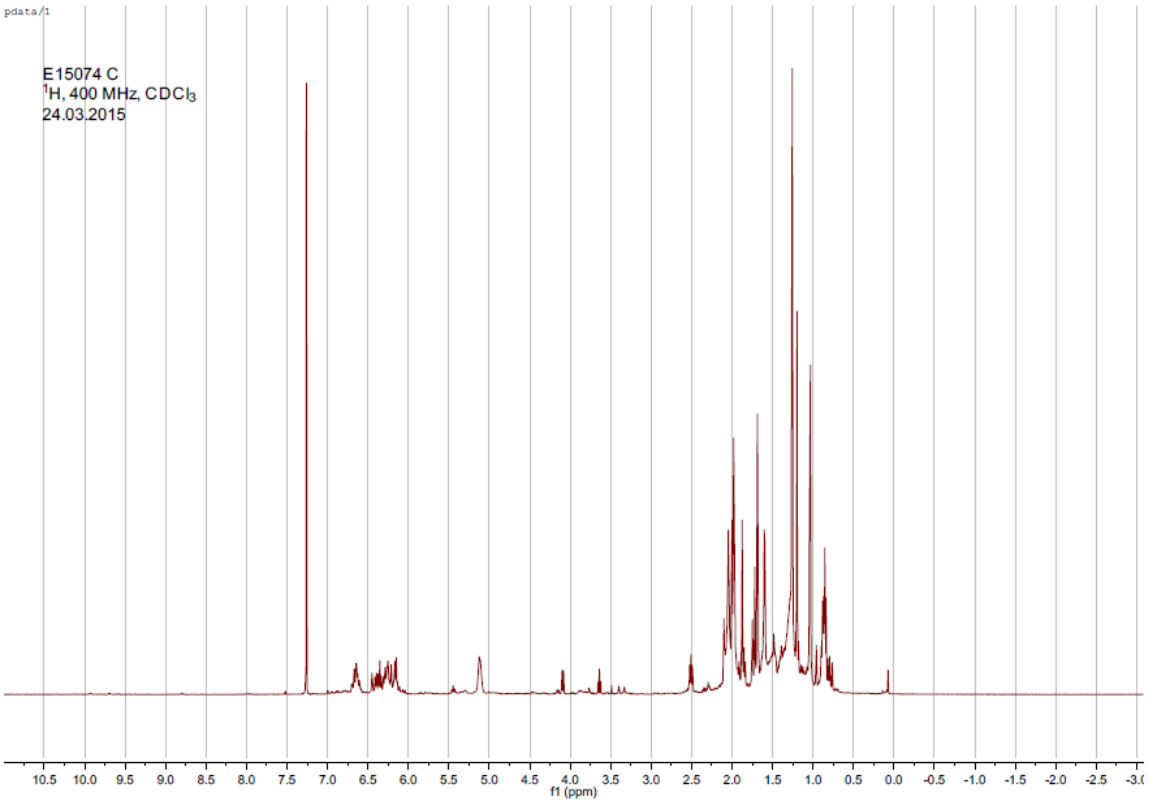

Figure 21 Fraction C.

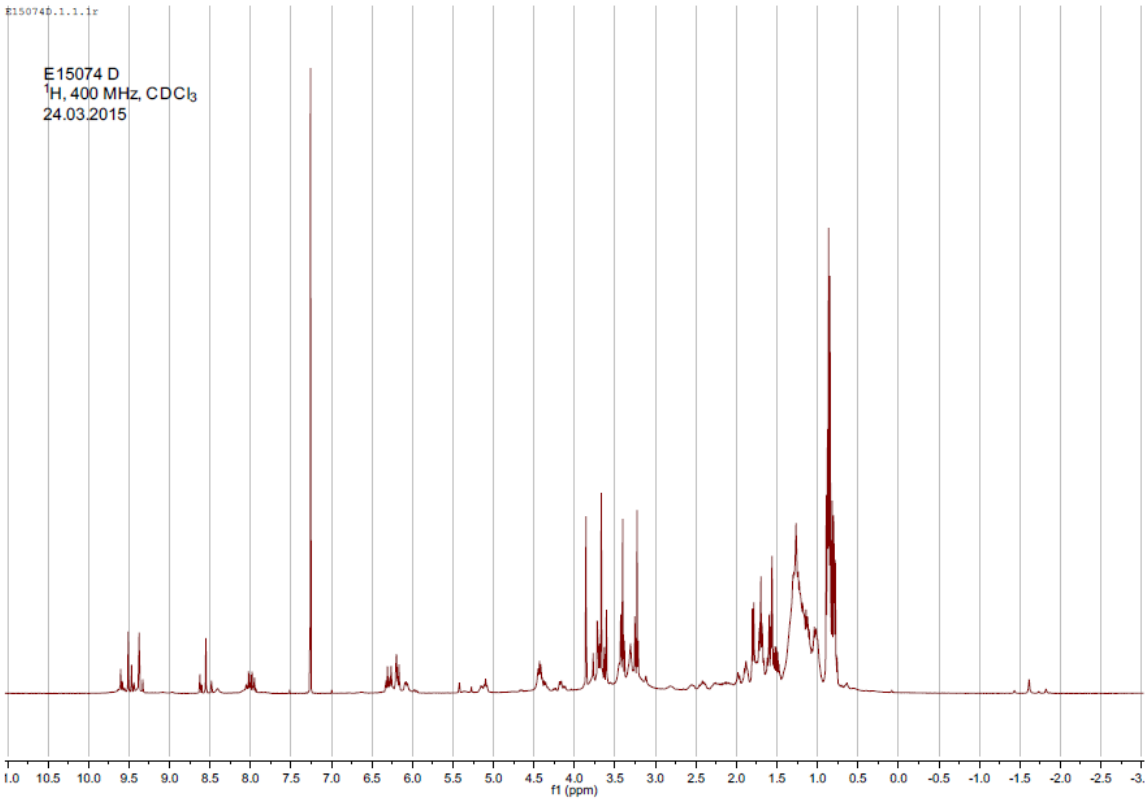

Figure 22 Fraction D.

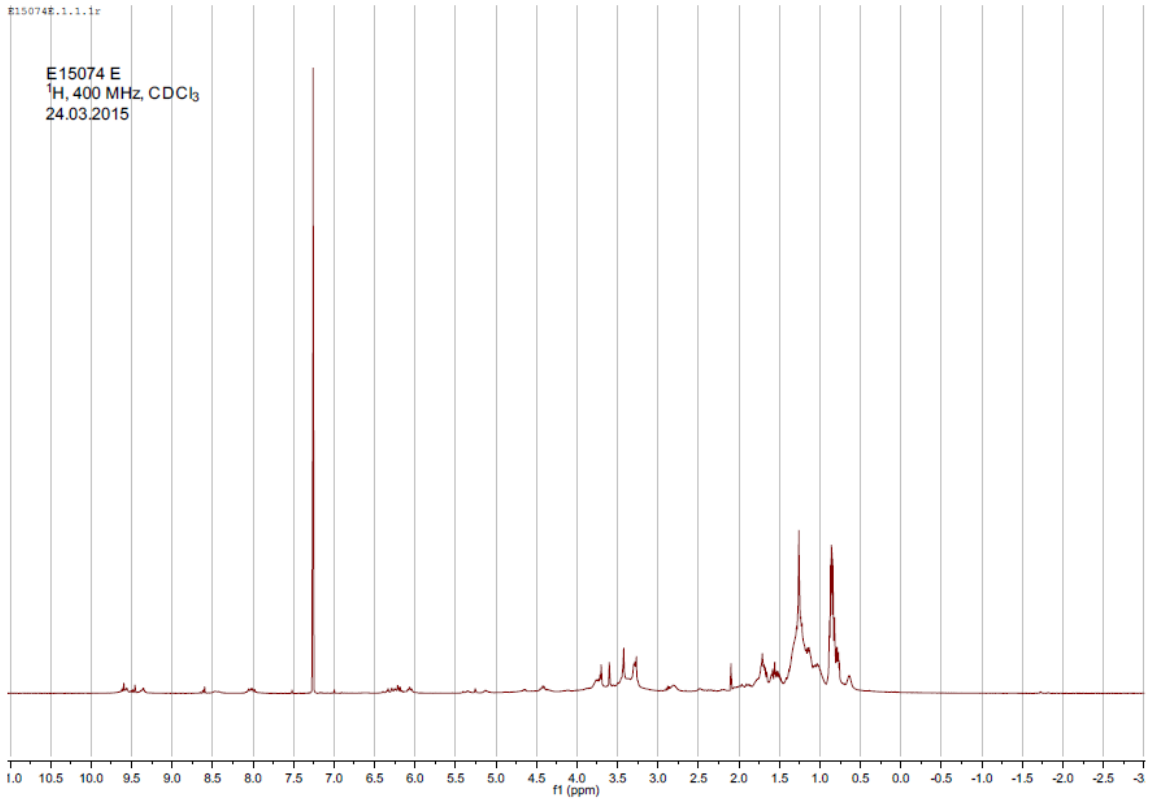

Figure 23 Fraction E.

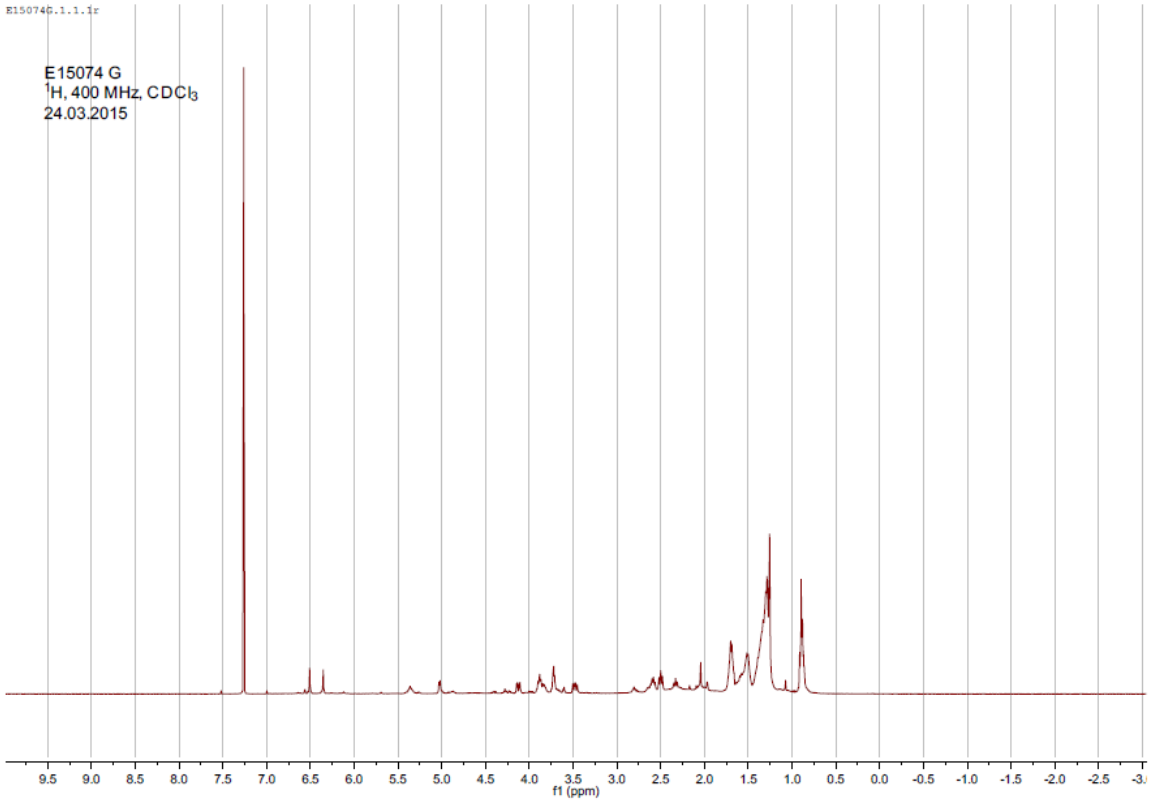

Figure 24 Fraction G.

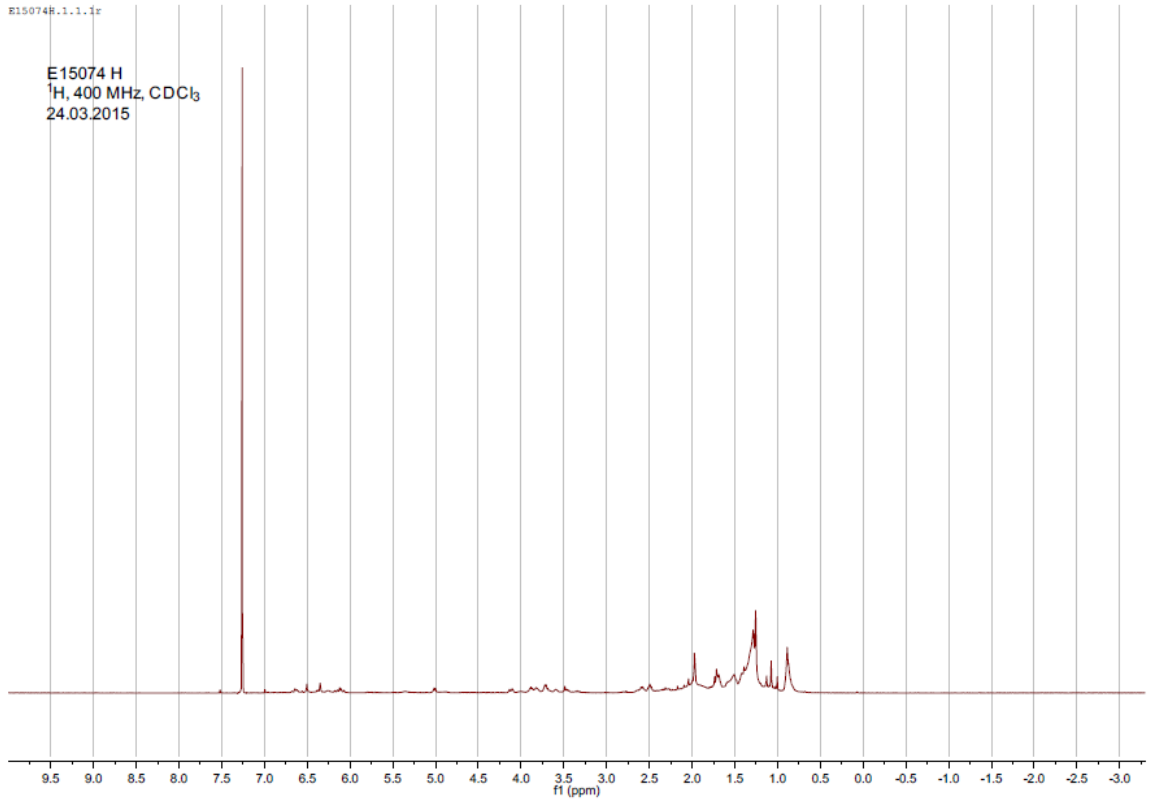

Figure 25 Fraction H.

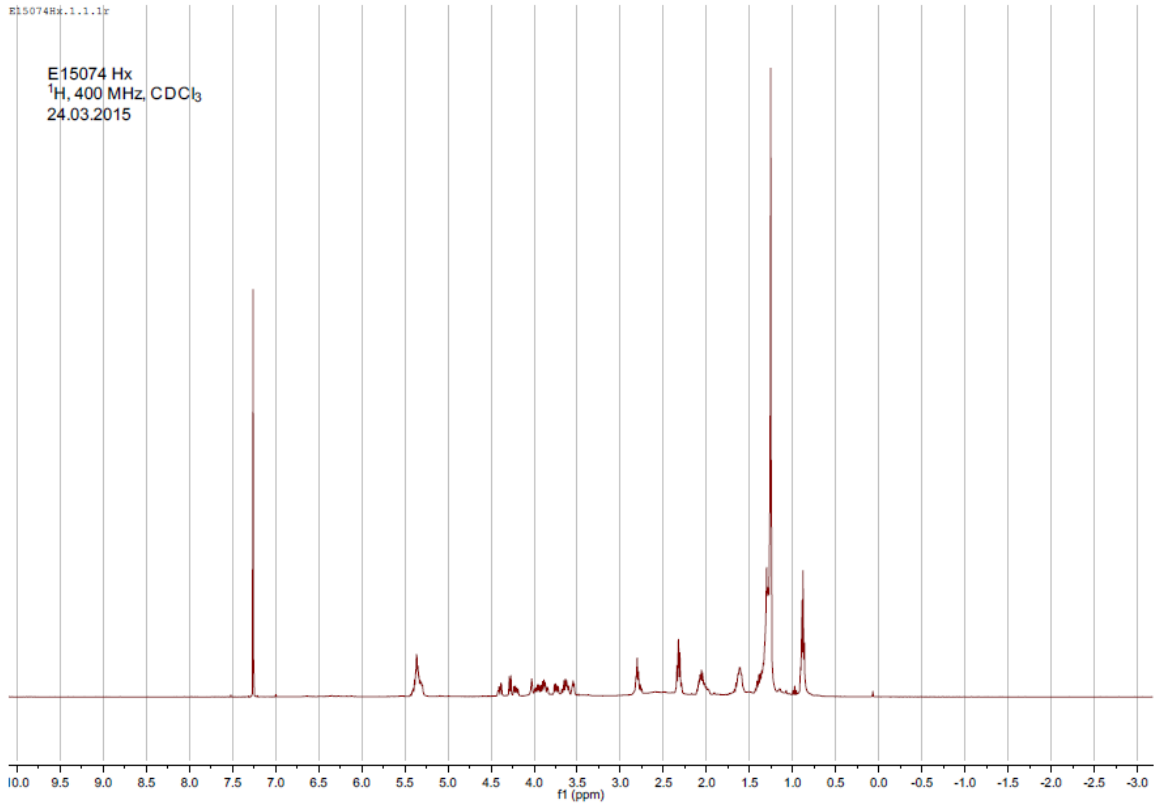

Figure 26 Fraction Hx.

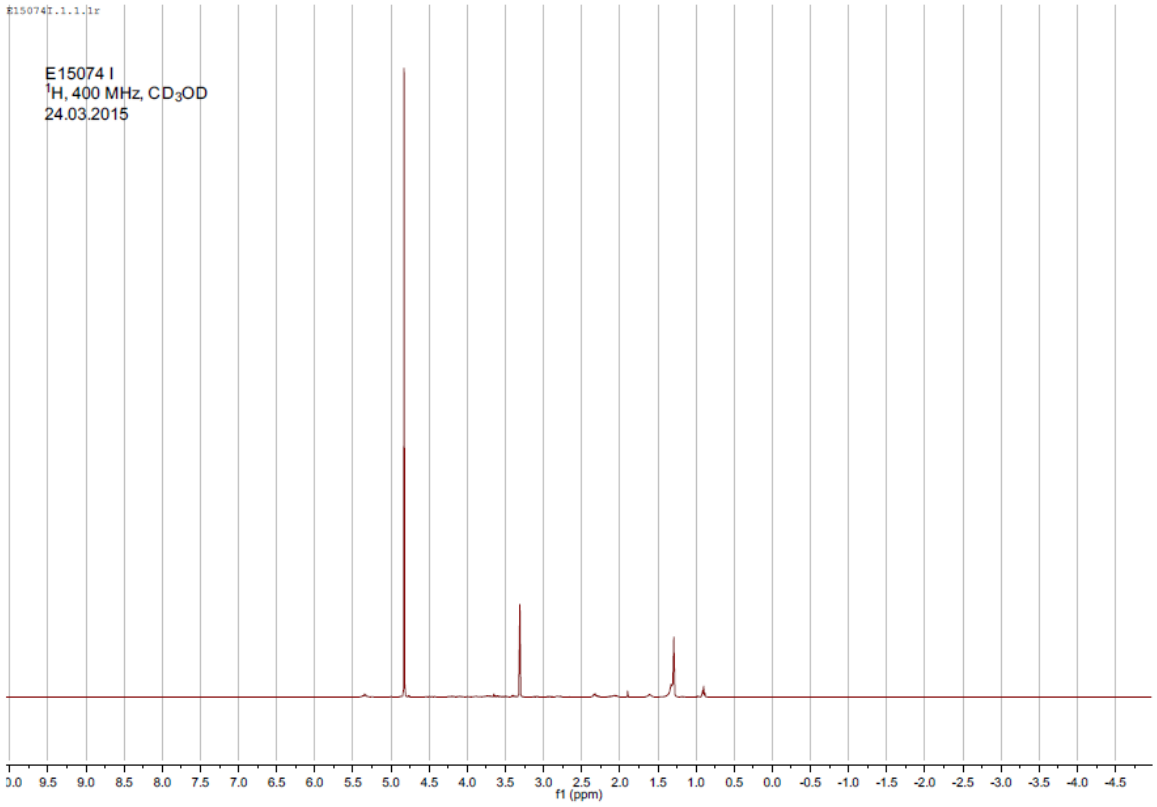

Figure 27 Fraction I.

Appendix 2 – Thin Layer Chromatography

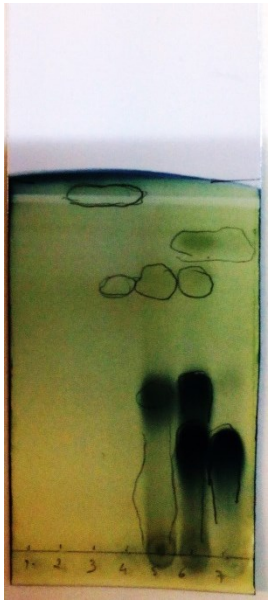

Figure 28 Sub-Fraction 1 – 7.

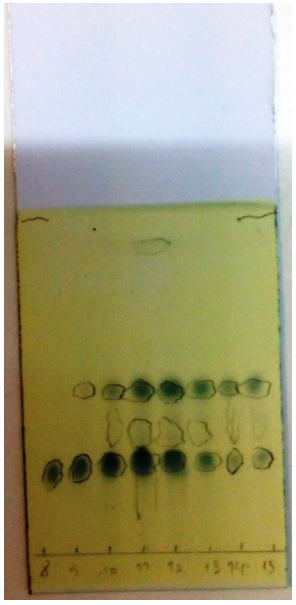

Figure 29 Sub-Fraction 8 – 15.

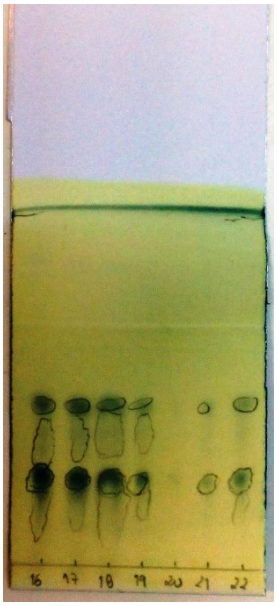

Figure 30 Sub-Fraction 16 – 22.

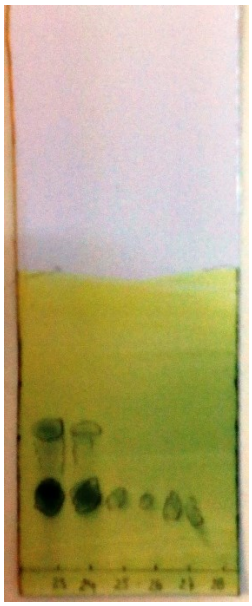

Figure 31 Sub-Fraction 23 – 28.

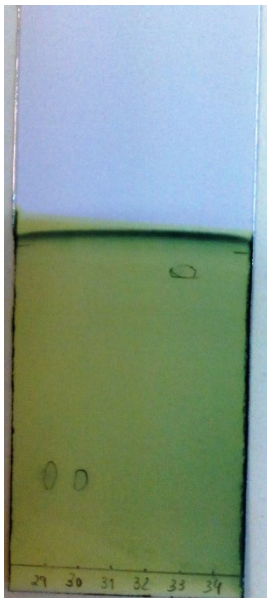

Figure 32 Sub-Fraction 29 – 34.

Figure 33 Sub-Fraction 35 – 41.

Figure 34 Sub-Fraction 42 – 47.

Figure 35 Sub-Fraction 48 – 53.

Figure 36 Sub-Fraction 54 – 59.

Figure 37 Sub-Fraction 60 – 65.

Figure 38 Sub-Fraction 66 – 72.

Figure 39 Sub-Fraction 73 – 75.

Appendix 3 – Exposure to compound and cytotoxicity assays

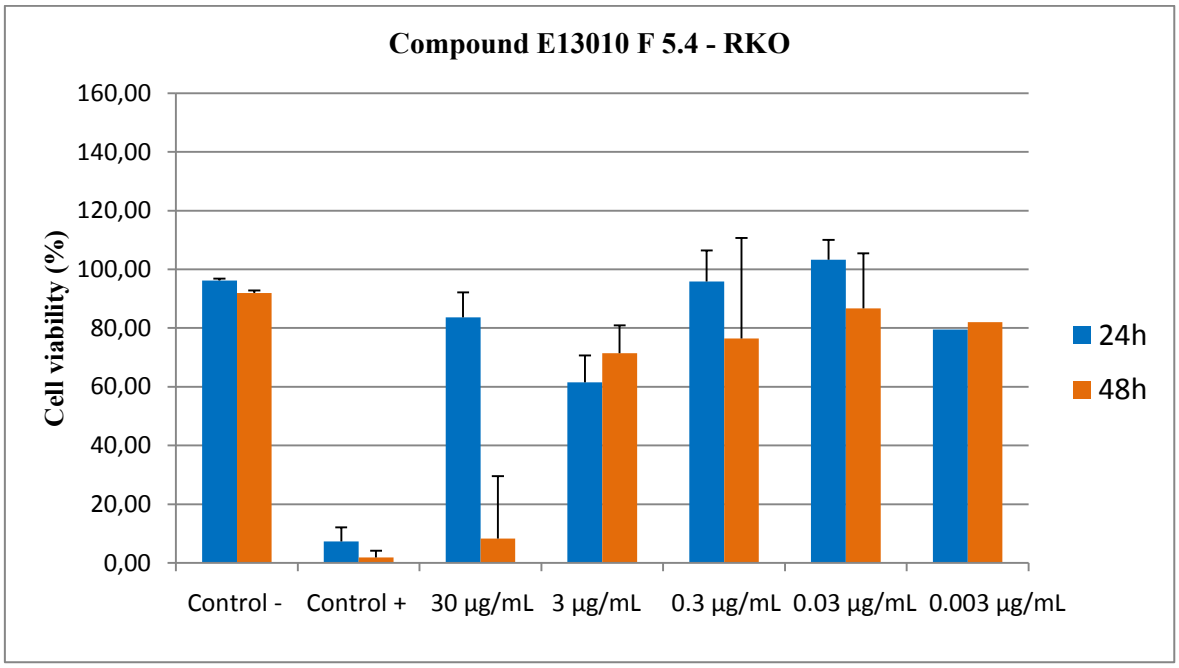

Figure 40 Cell viability from compound E13010 F 5.4 of the cyanobacterial strain LEGE06099, in the RKO tumour cell line, at a concentration 30 µg/mL, 3 µg/mL, 0.3 µg/mL, 0.03 µg/mL, 0.003 µg/mL, with exposure time of 24 and 48 hours at $3.3x10^4$ cells per well. The negative control corresponds to 1% DMSO (50 µL) and the positive control to 20% DMSO (100 µL).

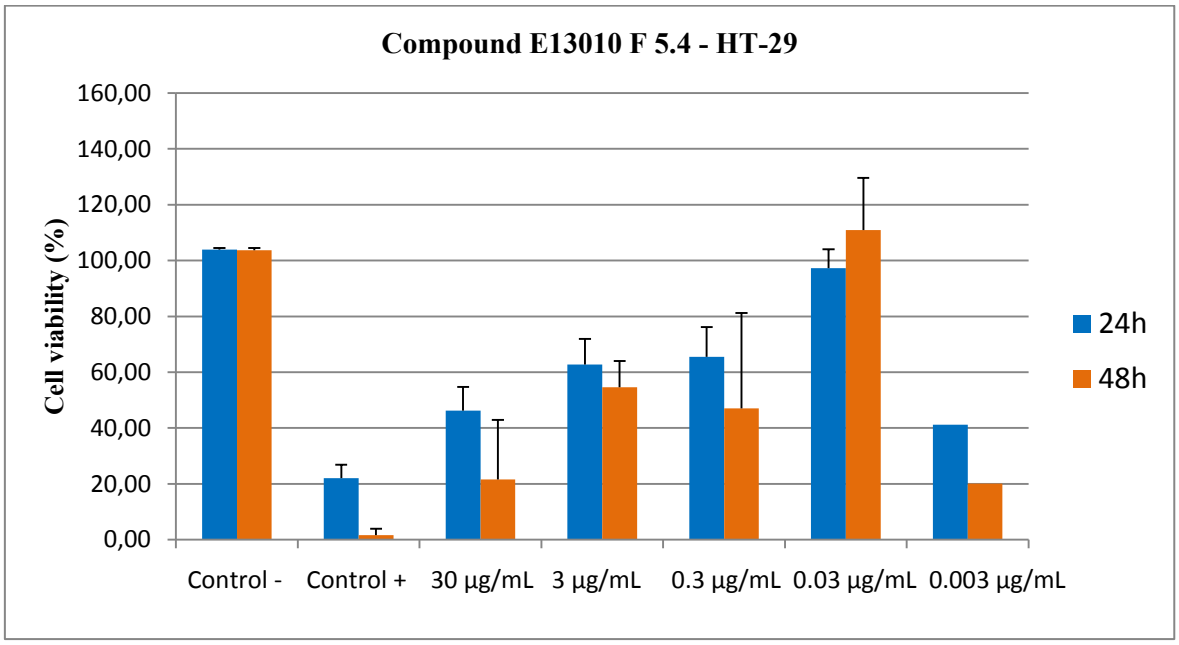

Figure 41 Cell viability from compound E13010 F 5.4 of the cyanobacterial strain LEGE06099, in the HT-29 tumour cell line, at a concentration 30 µg/mL, 3 µg/mL, 0.3 µg/mL, 0.03 µg/mL, 0.003 µg/mL, with exposure time of 24 and 48 hours at $3.3x10^4$ cells per well. The negative control corresponds to 1% DMSO (12 µL) and the positive control to 20% DMSO (100 µL).

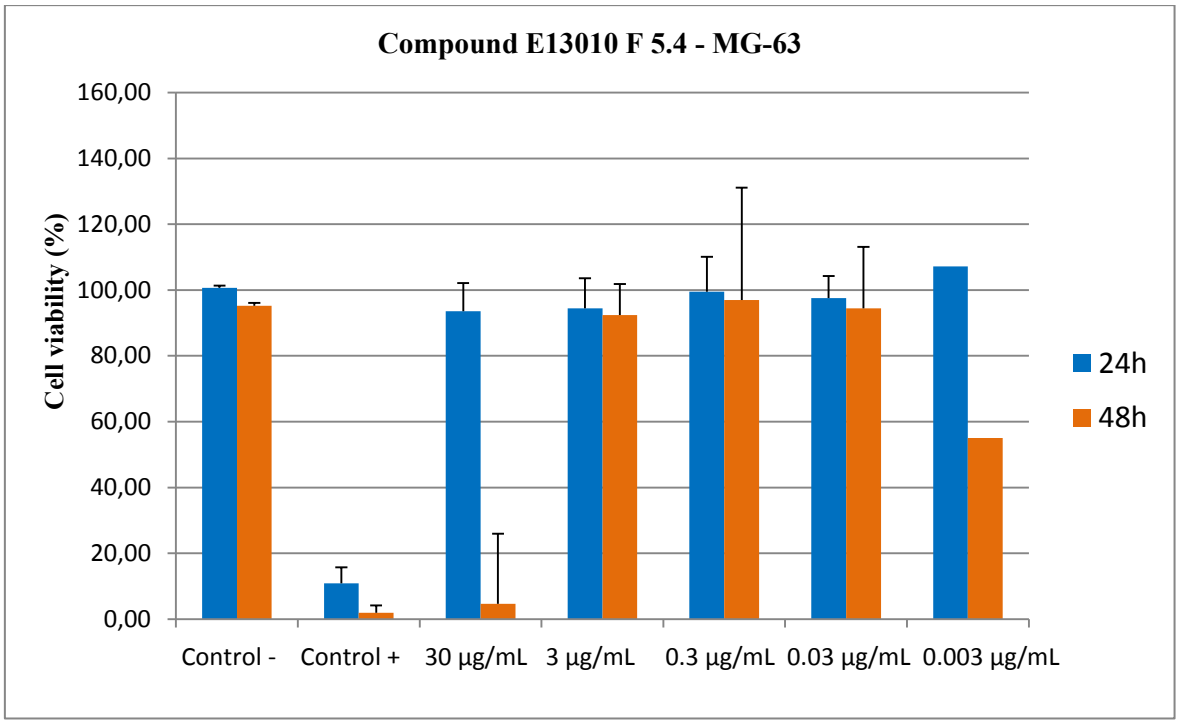

Figure 42 Cell viability from compound E13010 F 5.4 of the cyanobacterial strain LEGE06099, in the MG-63 tumor cell line, at a concentration 30 µg/mL, 3 µg/mL, 0.3 µg/mL, 0.03 µg/mL, 0.003 µg/mL, with exposure time of 24 and 48 hours at $3.3x10^4$ cells per well. The negative control corresponds to 1% DMSO (50 µL) and the positive control to 20% DMSO (100 µL).

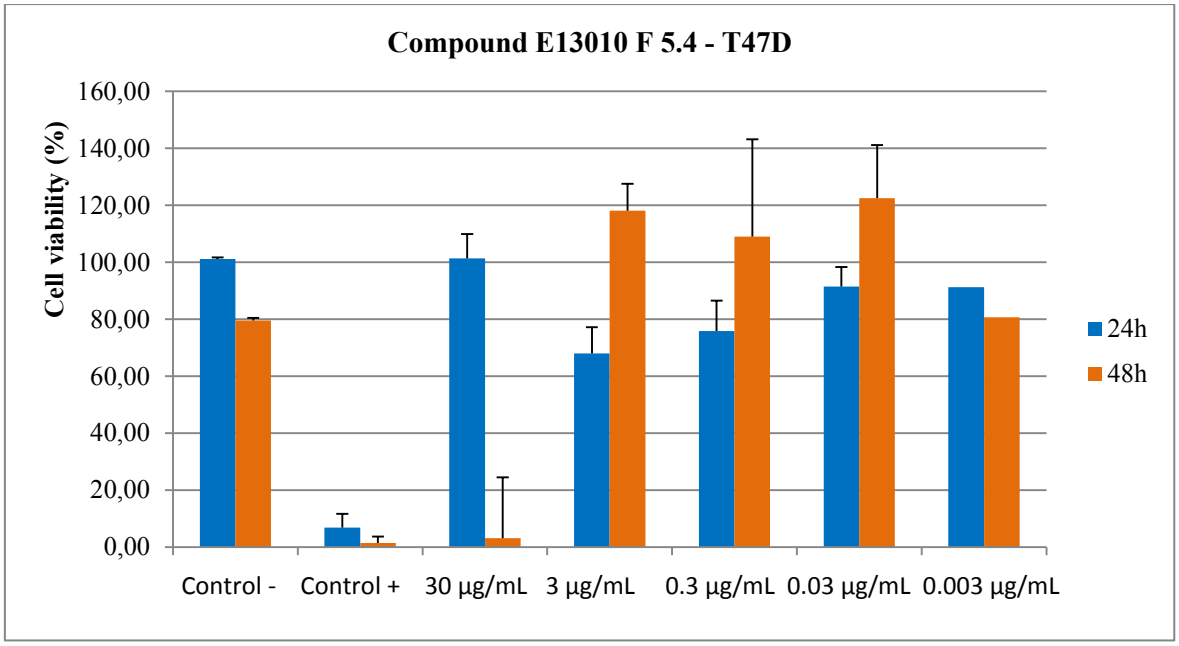

Figure 43 Cell viability from the compound E13010 F 5.4 of the cyanobacterial strain LEGE06099, in the T47D tumour cell line, at a concentration 30 µg/mL, 3 µg/mL, 0.3 µg/mL, 0.03 µg/mL, 0.003 µg/mL, with exposure time of 24 and 48 hours at $3.3x10^4$ cells per well. The negative control corresponds to 1% DMSO (50 µL) and the positive control to 20% DMSO (100 µL).

Appendix 4 – Quantification of RNA

Table 11 Quantification of RNA with the *Qubit® Fluorometer* (Invitrogen).

Sample		Concentration (µg/mL)
RKO	Replicate 1 treated with compound	59,8
	Replicate 2 treated with compound	522
	Replicate 3 treated with compound	394
	Replicate 4 treated with compound	415
	Replicate 5 treated with compound	257
	Replicate 6 treated with compound	467
	Replicate 1 for Control –	108
	Replicate 2 for Control –	459
	Replicate 3 for Control –	475
	Replicate 4 for Control –	523
	Replicate 5 for Control –	298
	Replicate 6 for Control –	296
HT-29	Replicate 3 treated with compound	104
	Replicate 4 treated with compound	365
	Replicate 5 treated with compound	168
	Replicate 6 treated with compound	219
	Replicate 3 for Control –	11
	Replicate 4 for Control –	194
	Replicate 5 for Control –	184
	Replicate 6 for Control –	296

Appendix 5 – Results of Real Time PCR

Table 12 VDAC gene and geometric mean of RPL8 and HPRT1 genes.

Sample		Mean E(n)	Standard deviation E(n)
RKO	Fraction F 2	1.9	0.37
	Fraction F 3	0.4	0.40
	Fraction F 4	0.8	0.75
	Fraction F 5	1.4	1.08
	Fraction F 6	1.0	0.28
	Control – 1	0.9	0.11
	Control – 2	0.7	0.04
	Control – 3	0.9	0.15
	Control – 4	1.8	0.60
	Control – 5	0.9	0.07
	Control – 6	1.4	0.82
HT-29	Fraction F 3	2.4	0.11
	Fraction F 4	1.9	0.08
	Fraction F 5	1.0	0.49
	Fraction F 6	2.1	1.03
	Control – 4	1.3	0.63
	Control – 5	0.9	0
	Control – 6	0.9	0.43

Table 13 SHMT2 gene and geometric mean of RPL8 and HPRT1 genes.

Sample		Mean E(n)	Standard deviation E(n)
RKO	Fraction F 2	1.7	0.85
	Fraction F 3	0.6	0.27
	Fraction F 4	1.2	0.46
	Fraction F 5	0.7	0.03
	Fraction F 6	1.6	1.41
	Control – 1	0.7	0.01
	Control – 2	1.2	0.29
	Control – 3	1.5	0.01
	Control – 4	2.4	1.54
	Control – 5	0.9	0
	Control – 6	0.4	0.17
HT-29	Fraction F 3	0.7	0.14
	Fraction F 4	2.5	0.34
	Fraction F 5	0.8	0
	Fraction F 6	2.2	1.44
	Control – 4	1.2	0.56
	Control – 5	1.2	0.14
	Control – 6	0.8	0.30

Table 14 CCNE gene and geometric mean of RPL8 and HPRT1 genes.

Sample		Mean E(n)	Standard deviation E(n)
RKO	Fraction F 2	1.4	0.77
	Fraction F 3	0.5	0
	Fraction F 4	0.6	0.36
	Fraction F 5	0.8	0.52
	Fraction F 6	1.8	0.02
	Control – 1	1.0	0.03
	Control – 2	1.1	0.34
	Control – 3	1.4	0.41
	Control – 4	1.5	0.05
	Control – 5	0.9	0.18
	Control – 6	0.6	0.46
HT-29	Fraction F 3	1.0	0.27
	Fraction F 4	2.2	1.79
	Fraction F 5	1.0	0.92
	Fraction F 6	2.3	0.93
	Control – 4	1.0	0.37
	Control – 5	1.6	0.57
	Control – 6	0.7	0.47

Table 15 CCNB1 gene and geometric mean of RPL8 and HPRT1 genes.

Sample		Mean E(n)	Standard deviation E(n)
RKO	Fraction F 2	1.5	0.50
	Fraction F 3	2.8	1.40
	Fraction F 4	0.9	0.14
	Fraction F 5	1.6	0.24
	Fraction F 6	0.8	0.04
	Control – 1	0.8	0.07
	Control – 2	0.6	0.02
	Control – 3	0.9	0.03
	Control – 4	1.7	0.14
	Control – 5	1.2	0.15
	Control – 6	1.0	0.13
HT-29	Fraction F 3	2.5	1.29
	Fraction F 4	2.1	0.87
	Fraction F 5	1.4	0.64
	Fraction F 6	1.0	0.15
	Control – 4	1.6	0.49
	Control – 5	0.9	0.48
	Control – 6	1.0	0.75

Table 16 P21CIP gene and geometric mean of RPL8 and HPRT1 genes.

Sample		Mean E(n)	Standard deviation E(n)
RKO	Fraction F 2	0.5	0.02
	Fraction F 3	0.3	0.08
	Fraction F 4	0.6	0.14
	Fraction F 5	0.1	0.10
	Fraction F 6	0.9	0.38
	Control – 1	1.0	0.02
	Control – 2	1.5	0.21
	Control – 3	1.4	0
	Control – 4	1.3	0.33
	Control – 5	1.1	0.06
	Control – 6	0.3	0.07
HT-29	Fraction F 3	0.8	0.08
	Fraction F 4	2.8	0.42
	Fraction F 5	1.7	0.11
	Fraction F 6	2.7	0.73
	Control – 4	0.9	0.22
	Control – 5	1.2	0.39
	Control – 6	1.1	0.60

Table 17 BCL-2 gene and geometric mean of RPL8 and HPRT1 genes.

Sample		Mean E(n)	Standard deviation E(n)
RKO	Fraction F 2	1.7	0.67
	Fraction F 3	0.9	0.37
	Fraction F 4	1.3	0.44
	Fraction F 5	1.5	0.71
	Fraction F 6	0.6	0.42
	Control – 1	0.5	0.23
	Control – 2	0.8	0.12
	Control – 3	0.9	0.43
	Control – 4	1.8	0.88
	Control – 5	1.2	0.16
	Control – 6	1.5	0.78
HT-29	Fraction F 3	1.1	0.22
	Fraction F 4	3.8	1.90
	Fraction F 5	2.7	1.86
	Fraction F 6	1.3	0.50
	Control – 4	0.9	0.49
	Control – 5	1.2	0.18
	Control – 6	1.2	0.86

Table 18 BAD gene and geometric mean of RPL8 and HPRT1 genes.

Sample		Mean E(n)	Standard deviation E(n)
RKO	Fraction F 2	0.8	0.09
	Fraction F 3	0.6	0.02
	Fraction F 4	0.6	0.02
	Fraction F 5	0.2	0
	Fraction F 6	0.8	0.33
	Control – 1	0.8	0.26
	Control – 2	1.7	0.25
	Control – 3	2.2	0.13
	Control – 4	1.1	0.13
	Control – 5	1.1	0.06
	Control – 6	0.3	0.07
HT-29	Fraction F 3	0.5	0.01
	Fraction F 4	2.1	0.01
	Fraction F 5	0.8	0.09
	Fraction F 6	1.1	0.19
	Control – 4	1.2	0.26
	Control – 5	1.8	1.58
	Control – 6	0.7	0.49

Appendix 6 – Protein concentration

Table 19 Protein concentration obtained from each samples of RKO and HT-29 cells line exposed to compound, according to the extraction protocol.

Sample		[Protein] µg/µL
RKO	Replicate 1 treated with compound	3.60
	Replicate 2 treated with compound	2.93
	Replicate 3 treated with compound	3.43
	Replicate 4 treated with compound	2.96
	Replicate 5 treated with compound	2.79
	Replicate 6 treated with compound	3.87
	Replicate 1 for Control –	5.97
	Replicate 2 for Control –	4.38
	Replicate 3 for Control –	4.47
	Replicate 4 for Control –	3.34
	Replicate 5 for Control –	3.03
	Replicate 6 for Control –	2.83
HT-29	Replicate 1 treated with compound	2.71
	Replicate 2 treated with compound	2.52
	Replicate 3 treated with compound	2.02
	Replicate 4 treated with compound	2.00
	Replicate 5 treated with compound	4.10
	Replicate 6 treated with compound	4.59
	Replicate 1 for Control –	4.42
	Replicate 2 for Control –	2.56
	Replicate 3 for Control –	2.29
	Replicate 4 for Control –	6.43
	Replicate 5 for Control –	1.40
	Replicate 6 for Control –	1.67

Appendix 7 – Relative intensity of the spots

Table 20 Relative intensity of the spots differentially expressed in the cell line RKO, detected by *PDQuest* software based on t-test at 95% confidence. Representation for each spot, considering the control group and treatment, the average relative intensity and respective standard deviation.

SSP	Control – (Mean ± SD)	Compound (Mean ± SD)
1603	1151.9 ± 366.7	475.6 ± 356.3
2303	17077.8 ± 3623.8	9011.9 ± 7516.3
2707	16469.4 ± 2056.5	7328 ± 3872.3
-++3303	1664.9 ± 445.1	710 ± 578.9
3313	32.1 ± 0.0	204.4 ± 121.1
3405	86.6 ± 49.5	544.1 ± 333.8
3517	110.7 ± 132.9	393.1 ± 209.4
3520	---	738.3 ± 355.2
3831	---	137.5 ± 42
3832	89.3 ± 62.8	277.3 ± 85.3
3844	---	164.3 ± 65.1
4303	135.9 ± 103.6	396.8 ± 110.6
4314	37 ± 34,3	615.9 ± 427.6
4415	167 ± 102.0	354.3 ± 78.2
4510	1831.5 ± 444.6	4014.9 ± 1692.1
4518	310.1 ± 172.6	1802.4 ± 668
4603	21.1 ± ---	427.1 ± 164.4
4905	---	158.9 ± 66.8
4906	62.9 ± 1.1	102.5 ± 4.8
5115	54.8 ± 14.2	14.5 ± 13.1
5214	133.9 ± 56.7	341.2 ± 107.7
5413	70.1 ± 43	160.9 ± 49.4
5415	147.6 ± 49.5	362.2 ± 159.4
5505	690.1 ± 178.3	1330.6 ± 403.1
5518	40.5 ± 26.5	278.6 ± 44.2
6101	791.4 ± 342.9	314.8 ± 139.8
6114	76.2 ± 11.4	132.9 ± 27.1
6208	120.1 ± 46.9	45.5 ± 20.3
6304	21675.6 ± 3354.5	14497.9 ± 3316.4
7102	3764.6 ± 416.2	2724.5 ± 740
7701	883.7 ± 159.1	629.9 ± 94.3
7807	513.3 ± ---	579.1 ± 39
8016	73.1 ± 27.1	22.6 ± 7.3
8111	127.8 ± 143.9	1002 ± 492.5
9907	---	911.9 ± 704

Table 21 Relative intensity of the spots differentially expressed in the cell line HT-29, detected by *PDQuest* software based on t-test at 95% confidence. Representation for each spot, considering the control group and treatment, the average relative intensity and respective standard deviation.

SSP	Control – (Mean ± SD)	Compound (Mean ± SD)
105	172.8 ± 104.4	625.8 ± 339.9
202	322.7 ± 201	861.8 ± 227.6
302	385.5 ± 185.6	722.5 ± 94.1
1208	---	296.6 ± 77.5
2411	9511.3 ± 5830.3	28137.6 ± 8476.7
2506	422 ± 213	1076.4 ± 306.9
2605	647 ± 339	1460 ± 251.7
2911	79.4 ± 35.06	184.2 ± 50.4
3301	197 ± 129.3	---
4407	386 ± 140.2	1874.2 ± 1115.9
4501	531.2 ± 75.3	---
5101	133.2 ± 63.7	289.6 ± 58.6
5103	119.3 ± 72.2	346 ± 91.2
5304	101.9 ± 80.9	304.7 ± 68.8
5403	353.9 ± 161.4	635.8 ± 75.6
5502	95.2 ± 38.4	79.8 ± ---
5505	155.1 ± 58	301.7 ± 64.4
5507	126.8 ± 59.5	453.5 ± 177.7
5610	133.5 ± 83.5	480.1 ± 143
5813	19.2 ± 10.8	153.9 ± 71.4
6101	624.9 ± 294.6	1180 ± 354.5
6103	---	431.9 ± 54
6201	213.5 ± 157.1	541.4 ± 118
6412	186.8 ± 78.9	440.8 ± 184.2
6502	192.1 ± 91.6	406.4 ± 123
6809	158.5 ± 137.1	711.2 ± 260.3